



**HAL**  
open science

## Modulation of spike-timing dependent plasticity: towards the inclusion of a third factor in computational models

Alexandre Foncelle, Alexandre Mendes, Joanna Jedrzejewska-Szmek, Silvana Valtcheva, Hugues Berry, Kim T. Blackwell, Laurent Venance

### ► To cite this version:

Alexandre Foncelle, Alexandre Mendes, Joanna Jedrzejewska-Szmek, Silvana Valtcheva, Hugues Berry, et al.. Modulation of spike-timing dependent plasticity: towards the inclusion of a third factor in computational models. *Frontiers in Computational Neuroscience*, In press, 12, pp.49. 10.3389/fn-com.2018.00049 . hal-01809075v1

**HAL Id: hal-01809075**

**<https://inria.hal.science/hal-01809075v1>**

Submitted on 6 Jun 2018 (v1), last revised 3 Jul 2018 (v2)

**HAL** is a multi-disciplinary open access archive for the deposit and dissemination of scientific research documents, whether they are published or not. The documents may come from teaching and research institutions in France or abroad, or from public or private research centers.

L'archive ouverte pluridisciplinaire **HAL**, est destinée au dépôt et à la diffusion de documents scientifiques de niveau recherche, publiés ou non, émanant des établissements d'enseignement et de recherche français ou étrangers, des laboratoires publics ou privés.

# Modulation of spike-timing dependent plasticity: towards the inclusion of a third factor in computational models

Alexandre Foncele<sup>1</sup>, Alexandre Mendes<sup>2</sup>, Joanna Jedrzejewska-Szmek<sup>3</sup>, Silvana Valtcheva<sup>2</sup>, Hugues Berry<sup>1</sup>, Kim Blackwell<sup>3</sup>, Laurent Venance<sup>2\*</sup>

<sup>1</sup>Inria Grenoble - Rhône-Alpes research centre, France, <sup>2</sup>Center for Interdisciplinary Research in Biology (CIRB), CNRS 7241 / INSERM U1050, INSERM U1050 Centre Interdisciplinaire de Recherche en Biologie, France, <sup>3</sup>Krasnow Institute for Advanced Study, United States

**Submitted to Journal:**

Frontiers in Computational Neuroscience

**Article type:**

Review Article

**Manuscript ID:**

374749

**Received on:**

15 Mar 2018

**Revised on:**

29 May 2018

**Frontiers website link:**

[www.frontiersin.org](http://www.frontiersin.org)

---

### ***Conflict of interest statement***

The authors declare that the research was conducted in the absence of any commercial or financial relationships that could be construed as a potential conflict of interest

### ***Author contribution statement***

AF and AM participate to the writing of the neuromodulators part; JJ, HB and KB wrote the "Molecular pathway-based computational models of STDP " part; SV wrote the "Modulation of STDP by astrocytes: the forgotten third factor " part; LV wrote the introduction, neuromodulators and conclusion parts; all authors have edited and corrected the ms.

### ***Keywords***

spike-timing dependent plasticity (STDP), Dopamine, noradrenaline, Astrocytes, Acetylcholine, BDNF, Hebbian plasticity, computational model, GABA Modulators, Eligibility Traces, third factor, credit assignment

### ***Abstract***

Word count: 267

In spike-timing dependent plasticity (STDP) change in synaptic strength depends on the timing of pre- versus postsynaptic spiking activity. Since STDP is in compliance with Hebb's postulate, it is considered one of the major mechanisms of memory storage and recall. STDP comprises a system of two coincidence detectors with NMDA receptor activation often posited as one of the main components. Numerous studies have unveiled a third component of this coincidence detection system, namely neuromodulation and glia activity shaping STDP. Even though dopaminergic control of STDP has most often been reported, acetylcholine, noradrenaline, nitric oxide, BDNF or GABA also has been shown to effectively modulate STDP. Furthermore, it has been demonstrated that astrocytes, via the release or uptake of glutamate, gate STDP expression. At the most fundamental level, the timing properties of STDP are expected to depend on the spatiotemporal dynamics of the underlying signaling pathways. However in most cases, due to technical limitations experiments grant only indirect access to these pathways. Computational models carefully constrained by experiments, allow for a better qualitative understanding of the molecular basis of STDP and its regulation by neuromodulators. Recently, computational models of calcium dynamics and signaling pathway molecules have started to explore STDP emergence in ex and in vivo-like conditions. These models are expected to reproduce better at least part of the complex modulation of STDP as an emergent property of the underlying molecular pathways. Elucidation of the mechanisms underlying STDP modulation and its consequences on network dynamics is of critical importance and will allow better understanding of the major mechanisms of memory storage and recall both in health and disease.

### ***Funding statement***

ANR Dopaciumcity (NEUC2014), INSERM, INRIA, Collège de France, Fondation pour la recherche Médicale (FRM).

1  
2  
3  
4  
5  
6  
7  
8  
9  
10  
11  
12  
13  
14  
15  
16  
17  
18  
19  
20  
21  
22  
23  
24

# **Modulation of spike-timing dependent plasticity: towards the inclusion of a third factor in computational models**

Alexandre Foncelle<sup>1,2\*</sup>, Alexandre Mendes<sup>3,4\*</sup>, Joanna Jędrzejewska-Szmek<sup>5</sup>, Silvana Valtcheva<sup>3,4</sup>, Hugues Berry<sup>1,2#</sup>, Kim T. Blackwell<sup>5#</sup>, Laurent Venance<sup>3,4#</sup>

1. INRIA, 56 Blvd Niels Bohr, Villeurbanne, France, F-69603
2. University of Lyon, LIRIS UMR 5205 CNRS-INSA, Villeurbanne, France, F-696213.
3. Center for Interdisciplinary Research in Biology, College de France, INSERM U1050, CNRS UMR7241, Labex Memolife, Paris, France;
4. University Pierre et Marie Curie, ED 158, Paris, France
5. The Krasnow Institute for Advanced Studies, George Mason University, Fairfax, VA, USA

#: Corresponding authors

Joanna Jędrzejewska-Szmek present address: Department of Neurophysiology, Nencki Institute of Experimental Biology, Warsaw, Poland

Silvana Valtcheva present address: Skirball Institute, Neuroscience Institute, Departments of Otolaryngology, Neuroscience and Physiology, New York University School of Medicine, New York, USA.

25 **Abstract**

26

27 In spike-timing dependent plasticity (STDP) change in synaptic strength depends on the  
28 timing of pre- *versus* postsynaptic spiking activity. Since STDP is in compliance with Hebb's  
29 postulate, it is considered one of the major mechanisms of memory storage and recall. STDP  
30 comprises a system of two coincidence detectors with NMDA receptor activation often  
31 posited as one of the main components. Numerous studies have unveiled a third component  
32 of this coincidence detection system, namely neuromodulation and glia activity shaping  
33 STDP. Even though dopaminergic control of STDP has most often been reported,  
34 acetylcholine, noradrenaline, nitric oxide, BDNF or GABA also has been shown to  
35 effectively modulate STDP. Furthermore, it has been demonstrated that astrocytes, *via* the  
36 release or uptake of glutamate, gate STDP expression. At the most fundamental level, the  
37 timing properties of STDP are expected to depend on the spatiotemporal dynamics of the  
38 underlying signaling pathways. However in most cases, due to technical limitations  
39 experiments grant only indirect access to these pathways. Computational models carefully  
40 constrained by experiments, allow for a better qualitative understanding of the molecular  
41 basis of STDP and its regulation by neuromodulators. Recently, computational models of  
42 calcium dynamics and signaling pathway molecules have started to explore STDP emergence  
43 in *ex* and *in vivo*-like conditions. These models are expected to reproduce better at least part  
44 of the complex modulation of STDP as an emergent property of the underlying molecular  
45 pathways. Elucidation of the mechanisms underlying STDP modulation and its consequences  
46 on network dynamics is of critical importance and will allow better understanding of the  
47 major mechanisms of memory storage and recall both in health and disease.

48

49 **Running title:** Modulation of STDP

50

51 **Keywords:** STDP, third factor, dopamine, acetylcholine, noradrenaline, astrocytes, eligibility  
52 traces, Hebbian plasticity, computational models

53

## 54 INTRODUCTION

55 Most computational and experimental studies of synaptic plasticity focus on  
56 variations of Hebb's rule in which the change in synaptic strength is caused by direct  
57 association of two factors, *i.e.* two inputs (or activity patterns), one on the presynaptic and  
58 one on the postsynaptic side. Thus, when neural circuits adjust their synaptic weights  
59 depending on the frequency or timing of the pre-synaptic and post-synaptic firing patterns,  
60 Hebb's postulate is fulfilled. In addition, a third factor (for example neuromodulators or  
61 astrocytes) stabilizes or modulates the expression of synaptic plasticity and, thus, ultimately  
62 learning (Kempster et al., 1998; Pawlak et al., 2010; Lisman et al., 2011; Frémaux and  
63 Gerstner, 2015; Edelman et al., 2017; Kusmierz et al., 2017; Gerstner et al., 2018). The  
64 inclusion of this third factor with two-factor Hebbian plasticity rule is called neoHebbian  
65 plasticity (Lisman et al., 2011), and is infrequent in computational models of STDP. In this  
66 review, we focus on spike-timing-dependent plasticity (STDP) (Sjöström et al., 2008;  
67 Feldman, 2012), a synaptic Hebbian learning rule, and its control by the third factor:  
68 neuromodulation (*via* the action of dopamine, acetylcholine, noradrenaline and others) or  
69 astrocyte activity. Our goal is to highlight aspects of STDP that should be taken into account  
70 in future computational models of STDP.

71 Since its discovery, STDP has attracted considerable interest in experimental and  
72 computational neuroscience because it avoids implausibly high firing frequencies and instead  
73 relies on spike correlation. STDP has emerged as a candidate mechanism for experience- and  
74 activity-dependent changes in neural circuits, including map plasticity (Abbott and Nelson,  
75 2000; Dan and Poo, 2006; Morrison et al., 2008; Sjöström et al., 2008; Feldman, 2012;  
76 Froemke, 2015). Experiments in different brain regions and in diverse neuronal types have  
77 revealed a plethora of STDP forms that vary in plasticity direction, temporal dependence and  
78 the involvement of signaling pathways (Sjöström et al., 2008; Feldman, 2012; Korte and  
79 Schmitz, 2016). Experimental protocols that investigate STDP use pairing of a presynaptic  
80 stimulation with a postsynaptic spike, with the pre- and postsynaptic stimulations separated  
81 by a fixed interval  $\Delta t_{\text{STDP}}$  (spike timing). In most of the studies, the spike timing is computed  
82 as  $\Delta t_{\text{STDP}} = t_{\text{post}} - t_{\text{pre}}$ , where  $t_{\text{post}}$  and  $t_{\text{pre}}$  are the times of emission of the postsynaptic spike and  
83 that of the presynaptic stimulation, respectively. If the postsynaptic stimulation occurs before  
84 the presynaptic,  $\Delta t_{\text{STDP}} < 0$  (post-pre pairings), whereas  $\Delta t_{\text{STDP}} > 0$  when the presynaptic  
85 stimulation occurs before the postsynaptic one (pre-post pairings). The same pairing pattern  
86 is then repeated between 50 and 200 times at a constant frequency (typically between 0.1 and

87 5Hz). The canonical STDP is bidirectional (able to generate potentiation and depression  
88 depending on the value of  $\Delta t_{\text{STDP}}$ ) and Hebbian, *i.e.* post-pre pairings ( $\Delta t_{\text{STDP}} < 0$ ) yield timing-  
89 dependent long-term depression (tLTD) and pre-post pairings ( $\Delta t_{\text{STDP}} > 0$ ) give rise to timing-  
90 dependent long-term potentiation (tLTP). For most STDP forms, the expression of plasticity  
91 is restricted to a narrow temporal window ( $|\Delta t_{\text{STDP}}| < 80\text{ms}$ ); thus, when pre- and postsynaptic  
92 activities are separated by a large  $\Delta t_{\text{STDP}}$ , long-term synaptic changes are not observed (Bi  
93 and Poo, 1998; Markram et al., 1997).

94 The predominant form of STDP is Hebbian, and has been observed in the neocortex  
95 (Feldman, 2000; Markram et al., 1997; Nevian and Sakmann, 2006; Sjöström et al., 2001;  
96 Froemke et al., 2005), the hippocampus (Debanne et al., 1997; Debanne et al., 1998; Bi and  
97 Poo, 1998; Nishiyama et al., 2000; Wittenberg and Wang, 2006), and the striatum (Shen et  
98 al., 2008; Pawlak and Kerr, 2008; Fino et al., 2008; Fino et al., 2009). In contrast to Hebbian  
99 STDP, bidirectional anti-Hebbian STDP expresses tLTP for  $\Delta t_{\text{STDP}} < 0$  and tLTD for  $\Delta t_{\text{STDP}} > 0$ .  
100 Anti-Hebbian STDP was first reported in the cerebellum-like structure of electrical fish (Bell  
101 et al., 1997). More recently, bidirectional anti-Hebbian STDP has been observed in mammals  
102 and in various structures including the striatum (Fino et al., 2005; Fino et al., 2010; Schulz et  
103 al., 2010; Paillé et al., 2013; Valtcheva et al., 2017) and the somatosensory cortex (Letzkus et  
104 al., 2006). Unidirectional anti-Hebbian forms of STDP inducing tLTD for both  $\Delta t_{\text{STDP}} < 0$  and  
105  $\Delta t_{\text{STDP}} > 0$ , have been observed in the cerebellum (Han et al., 2000; Safo and Regehr, 2008),  
106 the neocortex (Egger et al., 1999; Lu et al., 2007), the dorsal cochlear nucleus (Tzounopoulos  
107 et al., 2004), and the hippocampus (Wittenberg and Wang; 2006). Recently, a unidirectional  
108 Hebbian STDP where tLTP was observed for both post-pre and pre-post pairings, has been  
109 reported in hippocampus (Mishra et al., 2016). The mechanisms that produce these diverse  
110 forms of STDP are not completely understood, though could involve a third factor, such as  
111 neuromodulators (such as dopamine or acetylcholine) (for reviews see Pawlak et al., 2010;  
112 Edelman et al., 2017) or astrocytes.

113 All the forms of STDP described so far depend on one of three main systems of  
114 coincidence detectors (Feldman, 2012; Korte and Schmitz, 2016). The first system comprises  
115 the NMDA receptor (NMDAR) as the unique coincidence detector for both tLTP and tLTD,  
116 though voltage-sensitive calcium channels may play a role in coincidence detection. This  
117 form of plasticity has been reported in hippocampal CA1 neurons (Nishiyama et al., 2000),  
118 neocortical layer 2/3 pyramidal cells (Froemke et al., 2005), striatal output neurons (Pawlak  
119 and Kerr, 2008), and striatal GABAergic interneurons (Fino et al, 2008). The second system

120 combines NMDAR-dependent tLTP with tLTD which depends on metabotropic glutamate  
121 receptor (mGluR)- and/or cannabinoid type-1 receptor (CB<sub>1</sub>R)-activation. Though the tLTD  
122 is independent of postsynaptic NMDARs, the activation of presynaptic NMDARs can be  
123 implicated (Sjöström et al., 2003; Bender et al., 2006b; Corlew et al., 2007; Rodríguez-  
124 Moreno and Paulsen, 2008). This form of plasticity has been observed in the visual (layer  
125 2/3) and somatosensory (layer 5) cortex (Sjöström et al., 2003; Bender et al., 2006; Nevian  
126 and Sakmann, 2006; Corlew et al., 2007; Rodríguez-Moreno and Paulsen, 2008), cholinergic  
127 striatal interneurons (Fino et al., 2008) or striatal output neurons (Fino et al., 2010). Recently  
128 in striatal output neurons, a third system has been reported, in which the tLTD is CB<sub>1</sub>R-  
129 dependent, whereas the molecular dependence of tLTP is governed by the number of  
130 pairings: a small number of pairings (~10) produces a CB<sub>1</sub>R-mediated tLTP, whereas greater  
131 number of pairings yields an NMDAR-mediated tLTP (Cui et al., 2015; Cui et al., 2016).

132         The molecular mechanisms accounting for these various forms of STDP are not yet  
133 fully understood, despite a substantial number of studies focusing on STDP. For the  
134 NMDAR-dependent tLTP and tLTD, calcium amplitude seems to partly determine plasticity  
135 direction (Nevian and Sakmann, 2006). For  $\Delta t_{\text{STDP}} > 0$ , when the presynaptic activity precedes  
136 the back-propagating action potential, the excitatory post-synaptic potential coincides with  
137 the back-propagating action potential resulting in high and more prolonged calcium influx  
138 through the NMDAR and voltage-sensitive calcium channels, which leads to tLTP. For  
139  $\Delta t_{\text{STDP}} < 0$ , calcium influx through the NMDARs and voltage-sensitive calcium channels is  
140 lower and as a result induces tLTD (Magee and Johnston, 1997; Koester and Sakmann, 1998;  
141 Nevian and Sakmann, 2006; Pawlak and Kerr, 2008). These different calcium dynamics  
142 produce different directions of plasticity by recruiting different downstream signaling  
143 molecules. Several computational models have used a description of neuronal calcium  
144 dynamics and/or the kinetics of downstream signaling pathways as a proxy to predict the  
145 direction of plasticity (tLTP or tLTD). These computational models investigate the impact of  
146 different STDP timings or of modulators on STDP by integrating their effects on calcium  
147 dynamics or downstream signaling pathways. Therefore computational models based on the  
148 kinetics of the implicated molecular pathways are promising avenues to integrate the third  
149 factor in Hebbian plasticity and will be the main focus of the present review.

150

## 151 NEUROMODULATORS AFFECTING THE EXPRESSION, POLARITY AND 152 SHAPE OF STDP

153 Neuromodulators and neurotransmitters play an important, but often unappreciated,  
154 role in the control of STDP induction and maintenance (for reviews see Pawlak et al., 2010;  
155 Edelman et al., 2017). The skepticism about neuromodulation stems from the apparent  
156 discrepancy between the time scale of neuromodulation and the coincidence detection timing  
157 inherent to STDP. The former is on the scale of seconds or more, whereas the latter is on the  
158 scale of milliseconds. However, this apparent discrepancy becomes less important after  
159 considering STDP from the perspective of a learning system that needs to link recorded  
160 information (memory) with a value scale (reward). Indeed, an individual acting on its  
161 environment needs to learn to discriminate actions leading to reward from those leading to  
162 punishment, both possibly occurring seconds, minutes or even hours after the taken action. A  
163 system of memory and learning based only on the timescale of STDP would miss this  
164 essential information. Thus, one role of neuromodulation is to link STDP and the reward  
165 system. In this context, we demonstrate below how a third factor, comprised of  
166 neuromodulators and/or astrocytes, modulates the timing dependence of STDP. Note that the  
167 modulation of timing dependence depends on brain region and cell type; thus future  
168 computational models will need to incorporate region and cell type specific modulation. In  
169 this section, we detail STDP protocols used in experimental studies because depending on the  
170 activity patterns neuromodulatory systems are differentially recruited. Therefore, the apparent  
171 contradiction between several of the experimental reports on STDP could depend on the  
172 activity patterns or neuromodulatory activation that were used. This knowledge might help  
173 the building of computational models, by taking into account the different regimes of action  
174 of neuromodulators in shaping STDP.

175

### 176 **Dopamine**

177 The action of dopamine is mediated by the metabotropic dopaminergic receptors that  
178 functionally modulate other receptor systems and/or ion channels without inducing large  
179 postsynaptic currents. Dopaminergic receptors belong to two groups based on their G-protein  
180 coupling: the D<sub>1</sub>-class receptors (D<sub>1</sub>R and D<sub>5</sub>R) are coupled to G<sub>s</sub>- or G<sub>o1f</sub>-proteins and the  
181 D<sub>2</sub>-class receptors (D<sub>2</sub>R, D<sub>3</sub>R and D<sub>4</sub>R) to G<sub>i/o</sub>-proteins (Neve et al., 2004). D<sub>1</sub>- and D<sub>2</sub>-class  
182 receptors have opposite action on the cAMP second messenger pathway and the protein  
183 kinase A (Fig. 1a).

184 Dopamine is released by midbrain dopaminergic neurons in response to both reward  
185 and the reward prediction error (Schultz, 2007). In the hippocampus, tLTD, which is  
186 observed in control conditions for negative  $\Delta t_{\text{STDP}}$ , is converted to tLTP by dopamine  
187 addition during STDP pairings or immediately after STDP pairings (aiming at mimicking a  
188 retroactive effect) (Zhang et al., 2009; Brzosko et al., 2015) (Fig. 1b). Dopamine addition  
189 during STDP induction leads to the enlargement of the temporal window of tLTP expression  
190 (Fig. 1b). However the effects of dopamine disappear when dopamine is added long after  
191 STDP pairings, since dopamine addition 10 and 30 minutes after pairings results in an  
192 absence of plasticity and a recovery of tLTD observed in control conditions, respectively  
193 (Brzosko et al., 2015) (Fig. 1b). This dopaminergic modulation, which converts bidirectional  
194 STDP to unidirectional tLTP, is  $D_1R$ - but not  $D_2R$ -mediated (Zhang et al., 2009; Brzosko et  
195 al., 2015). Acetylcholine (classically associated with arousal and exploratory behavior; Ma et  
196 al., 2018) transforms bidirectional Hebbian hippocampal STDP into unidirectional tLTD  
197 (Brzosko et al., 2017). However, the effect of acetylcholine is reverted by dopamine addition  
198 1 second after STDP pairings, which allows recovering tLTP (Fig. 1b). Although these results  
199 constitute an important step for the experimental demonstration of a retroactive action of  
200 dopamine on Hebbian plasticity, the molecular mechanisms underlying dopamine interactions  
201 with the coincidence detectors were not characterized. In addition, more distal action of  
202 dopamine from STDP protocol remains to be investigated to fully explore the temporal  
203 credit-assignment problem (Sutton and Barto, 1998; Schultz, 2007; Izhikevich, 2007;  
204 Gerstner et al., 2018).

205 Additional evidence supports the role of dopamine for promoting hippocampal tLTP.  
206 Conditions that lower basal dopamine during the preparation of brain slices prevent the  
207 induction of tLTP at synapses between Shaffer collaterals and CA1 pyramidal cells  
208 (Edelmann and Lesmann, 2011). Subsequent addition of dopamine rescues tLTP, through a  
209  $D_1R$ -mediated mechanism (Edelmann and Lesmann, 2011; Edelmann and Lesmann, 2013).  
210 In addition,  $D_1$ - and  $D_5R$ -activations are important for the induction of tLTP at the synapses  
211 between the medial perforant pathway and dentate gyrus neurons (Yang and Dani, 2014). The  
212 mechanism here includes a change in cell excitability: inactivation of the transient A-type  
213 potassium current by  $D_1R$  and  $D_5R$  increases the excitability of dentate gyrus neurons and the  
214 amplitude of their back-propagating action potentials (Yang and Dani, 2014).

215 Beyond the hippocampus, the importance of dopamine modulation of STDP also is attested in  
216 the basal ganglia, where dopamine plays a crucial role in motor control, action selection and

217 reinforcement learning (Yin and Knowlton, 2006; Schultz, 2007). Given the importance of  
218 dopamine, it is not surprising that dopamine is required for STDP in the striatum, both *ex vivo*  
219 (Shen et al., 2008; Pawlak and Kerr, 2008) and *in vivo* (Schulz et al., 2010; Fisher et al.,  
220 2017). However, the situation is complicated by the diversity in dopamine receptors. In  
221 rodents, striatal output neurons belong either to the direct or the indirect trans-striatal  
222 pathways and show different dopaminergic receptor expression, D<sub>1</sub>- and D<sub>2</sub>-class receptors,  
223 respectively (Calabresi et al., 2014). *In vivo* in anesthetized rodents, negative and positive  
224 pairing STDP protocol both result in tLTD at corticostriatal synapses, and bidirectional STDP  
225 can be elicited only with phasic dopaminergic release obtained by electrical stimulation of  
226 midbrain dopaminergic neurons (Schulz et al., 2010) or pharmacological manipulation of  
227 dopaminergic transmission (together with GABAergic and adenosine transmissions) (Fisher  
228 et al., 2017). These results are consistent with *ex vivo* studies, which showed that application  
229 of dopamine either simultaneously, or 0.6 sec after glutamate allows dendritic spine  
230 enlargement and calcium increase (Yagishita et al., 2014). Moreover, this study demonstrated  
231 the existence of synaptic eligibility traces, which can be revealed by subsequent dopamine  
232 release after Hebbian learning (see section “Monoamines transform eligibility traces into  
233 plasticity” below). *Ex vivo*, conflicting results have been reported regarding STDP  
234 modulation by dopamine: according to Pawlak and Kerr (2008) both tLTD and tLTP requires  
235 D<sub>1</sub>R- but not D<sub>2</sub>R-activation (D<sub>2</sub>R-activation affecting only plasticity kinetics: tLTP and  
236 tLTD onset is shortened and delayed, respectively), whereas Shen et al. (2008) reported that  
237 D<sub>2</sub>R-activation is required for tLTD expression in striatal neurons belonging to the indirect  
238 pathway and D<sub>1</sub>R-activation is necessary for tLTP in striatal neurons belonging to the direct  
239 pathway. There are methodological differences between these two studies which could  
240 account for this discrepancy in results: for post-pre and pre-post pairings the same STDP  
241 protocol (*i.e.* 100 pairings at 0.1Hz) was applied by Pawlak and Kerr (2008), whereas two  
242 distinct STDP-like protocols (theta bursts 3:3 for tLTP and 1:3 for tLTD) were utilized by  
243 Shen et al. (2008). Depending on the activity patterns, D<sub>1</sub>- and D<sub>2</sub>-class receptors could be  
244 differentially activated. The effects of dopamine in the striatum via D<sub>2</sub>R receptors would  
245 result from a D<sub>2</sub>R-mediated attenuation of both synaptic- and back-propagating action  
246 potential-evoked calcium influx into dendritic spines *via* the inhibition of protein kinase A-  
247 dependent regulation of NMDARs (Higley and Sabatini, 2010) (Fig. 1). This mechanism also  
248 is supported by the demonstration that dopamine depletion enhances calcium influx in  
249 dendrites of the D<sub>2</sub>R-expressing striatal neurons belonging to the indirect pathway (Day et al.,  
250 2008). Future development of detailed computational models of the signaling pathways will

251 be useful for fully exploring the involvement of dopaminergic receptors in various forms of  
252 STDP (see section “Molecular pathway-based computational models of STDP”).

253 The role of dopamine has been demonstrated in two other brain regions, the prefrontal  
254 cortex and the amygdala. In the prefrontal cortex (at layer 5 pyramidal cells) an STDP  
255 protocol such as 60 pairings ( $\Delta t_{\text{STDP}} = +10\text{ms}$ ) at 0.1Hz fails to produce plasticity, while  
256 dopamine application during the STDP pairings permits the induction of Hebbian tLTP  
257 ( $\Delta t_{\text{STDP}} = +10\text{ms}$ ) (Xu and Yao, 2010) and anti-Hebbian tLTP ( $\Delta t_{\text{STDP}} = -30\text{ms}$ ) (Ruan et al.,  
258 2014) (Fig. 1b). Both Hebbian and anti-Hebbian tLTP directly depends upon  $D_1R$ -activation  
259 in the postsynaptic neuron whereas the Hebbian tLTP depends also indirectly upon the  
260 activation of  $D_2R$  expressed by GABAergic interneurons.  $D_2R$  activation blocks the  
261 inhibition exerted by GABAergic interneurons and permits the expression of Hebbian tLTP  
262 ( $\Delta t_{\text{STDP}} < +10\text{ms}$ ). By combining  $D_1R$ - and  $D_2R$ -activation, the temporal window of tLTP is  
263 extended up to  $\Delta t_{\text{STDP}} = +30\text{ms}$  (Xu and Yao, 2010) (Fig. 1c). This suggests that in prefrontal  
264 cortex, the physiological form of STDP is the anti-Hebbian tLTP since the expression of  
265 Hebbian tLTP is disfavored by GABAergic network activity. In the lateral nucleus of the  
266 amygdala tLTP requires the activation of  $D_2R$  located on neighboring GABAergic  
267 interneurons (Bissière et al., 2003). Since dopamine is released in the amygdala in response  
268 to stress (Inglis et al., 1999), dopaminergic neuromodulation of inhibitory synaptic  
269 transmission appears to be a crucial mechanism underlying the acquisition of fear  
270 conditioning.

271 In summary, these results show that dopamine is a key neuromodulator of STDP and  
272 constitutes the third factor required for the temporal credit-assignment. Overall, the effects of  
273 dopamine seem to conform to a simple general scheme: the activation of  $G_s/G_{\text{olf}}$ -coupled  $D_1R$   
274 tends to promote tLTP whereas the activation of  $G_i$ -coupled  $D_2R$  favors tLTD. However, the  
275 effects exerted by dopamine strongly depend on the brain area: dopamine either can be  
276 mandatory for STDP induction and/or maintenance or modulate STDP properties (width of  
277 the  $\Delta t_{\text{STDP}}$  window, polarity of the STDP or magnitude of the plasticity). Moreover, network  
278 effects can add complexity to the picture, since the expression of dopamine receptors is not  
279 restricted to the examined neuron but can affect the response to *e.g.* local interneurons.

280

## 281 **Noradrenaline**

282 Noradrenaline interacts with G-protein–coupled receptors of three families:  $\alpha$ 2-,  $\alpha$ 1-  
283 and  $\beta$ 1-3-adrenergic receptors (by order of decreasing affinity) (Ramos et al., 2007).  $\alpha$ 2-  
284 adrenergic receptors are Gi/Go-coupled and lead to cAMP decrease.  $\alpha$ 1-adrenergic receptors  
285 are Gq- coupled, and activate phospholipase C $\beta$ , resulting in intracellular calcium release via  
286 inositol 1,4,5-triphosphate.  $\beta$ -adrenergic receptors are Gs-coupled and yield cAMP increase  
287 (Fig. 2a).

288 In several brain regions, activation of adrenergic receptors modifies the shape of the  
289 STDP curve (Fig. 2b). In the hippocampus, activation of  $\beta$ -adrenergic receptors enlarges the  
290 range of  $\Delta t_{\text{STDP}}$  for Hebbian tLTP expression by increasing the excitability of CA1 pyramidal  
291 cells (Lin et al., 2003). In the visual cortex, whereas paired stimulations of layer 4 afferents  
292 with postsynaptic action potential bursts does not produce plasticity, the concomitant  
293 activation of adrenergic receptors (with both  $\alpha$ 1- and  $\beta$ -adrenergic receptor agonists) allows  
294 the emergence of bidirectional Hebbian STDP in pyramidal cells of layer 2/3 (in rodents: Guo  
295 et al., 2012; in primates: Huang et al., 2014) (Fig. 2b) as well as in fast-spiking interneurons  
296 and non-fast-spiking somatostatin-positive interneurons (Huang et al., 2013). Note that  $\alpha$ 1-  
297 adrenergic receptor agonists alone (or agonists of M<sub>1</sub>-class mAChRs, see section below; Seol  
298 et al., 2007) trigger a tLTD-only (*i.e.* unidirectional anti-Hebbian STDP), whereas  $\beta$ -  
299 adrenergic receptor agonists alone induce the expression of a tLTP-only (*i.e.* unidirectional  
300 Hebbian STDP) (Seol et al., 2007; Guo et al., 2012; Huang et al., 2013) (Fig. 2b). The  
301 affinity for noradrenaline of  $\alpha$ 1-adrenergic receptors exceeds that of  $\beta$ -adrenergic receptors,  
302 and unidirectional anti-hebbian STDP (tLTD-only) is observed in low noradrenaline, whereas  
303 bidirectional Hebbian STDP can be induced with higher noradrenaline concentration  
304 (Salgado et al., 2012) (Fig. 2b and 2c).

305 Taken together, those studies show that adrenergic receptors play an important role in  
306 shaping STDP, mostly by enlarging  $\Delta t_{\text{STDP}}$  and controlling STDP polarity, but also, similarly  
307 to dopamine, by acting subsequently to the stimulation to promote plasticity. Overall, a  
308 pattern emerges from the effects of noradrenaline: the activation of Gs-coupled  $\beta$ -adrenergic  
309 receptors tends to promote tLTP, whereas the activation of Gq-coupled  $\alpha$ 1-adrenergic  
310 receptors tends to favor tLTD.

311

## 312 **Monoamines transform eligibility traces into plasticity**

313 One of the fundamental questions in reward learning is the temporal credit-  
314 assignment problem: how are the correct actions learned given that delivery of a reward or  
315 punishment occurs significantly later than the key actions that promoted the outcome  
316 (Schultz, 2007). In an attempt to solve the temporal credit-assignment problem, some  
317 computational studies addressed the question of the retroactive effect of dopamine on cortical  
318 and hippocampal STDP (Sutton and Barto, 1998; Izhikevich, 2007; Gerstner et al., 2018).  
319 From a cellular perspective, the temporal credit-assignment problem translates into the  
320 following question: if dopamine (and more broadly monoamines) modulates STDP, is there a  
321 dependence of this modulation on the time elapsed between the stimulus (STDP pairings) and  
322 the reward (release of monoamines)? This question adds a supplementary temporal  
323 dimension to the modulation by the third-factor monoamine.

324 To solve the temporal credit-assignment or the distal reward problem, it has been  
325 proposed that synaptic eligibility traces could constitute synaptic tags that are set by  
326 Hebbian learning and that will be transformed subsequently into synaptic plasticity by  
327 neuromodulators, bridging the learning sequence with reward (Sutton and Barto, 1998;  
328 Izhikevich, 2007; Gerstner et al., 2018). In other words, eligibility traces would be induced  
329 by Hebbian learning but would remain silent in terms of synaptic efficacy changes, unless a  
330 neuromodulator released subsequently transforms them for plasticity. Synaptic eligibility  
331 traces would allow the synapse to keep a trace from the stimulus until getting the reward, the  
332 latter of which is represented by monoamines. We can distinguish two cases: the subsequent  
333 release of neuromodulator shapes an existing plasticity (Cassenaer and Laurent, 2012;  
334 Brzosko et al., 2015; Brzosko et al., 2017; Shindou et al., 2018) or allows the plasticity  
335 expression (Yagishita et al., 2014; He et al., 2015).

336 Octopamine, the equivalent of noradrenaline in insects, changes the bidirectional  
337 Hebbian STDP at synapses of Kenyon cells in the locust, critical for the associative learning  
338 of odors, into a unidirectional STDP (tLTD-only) even in a retroactive manner when applied  
339 seconds after the relevant pairing (Cassenaer and Laurent, 2012). In a similar way, in rodents,  
340 when dopamine is applied just after STDP pairings, it converts tLTD into tLTP in  
341 hippocampus (Brzosko et al., 2015; Brzosko et al., 2017) or in striatum (Shindou et al., 2018).

342 In striatum, dopamine induces spine enlargement exclusively when opto-stimulation  
343 of dopaminergic terminals occur between 0.3 to 2 seconds after Hebbian learning (*i.e.* STDP  
344 pairings) (Yagishita et al., 2014). In the visual cortex and in the medial prefrontal cortex,  
345 release of noradrenaline and serotonin, just after the whole set of pairings or just after every

346 pairing, allows the expression of tLTP and tLTD for pre-post and post-pre pairings,  
347 respectively (He et al., 2015); the STDP pairings *per se* did not induce plasticity (Fig. 2c). He  
348 et al. (2015) observed that the eligibility traces are short-lived since the monoamines need to  
349 be release 5 to 10 sec after learning to promote plasticity (He et al., 2015). The fact that a  
350 couple of monoamines (or third factors) is at play for distinct induction plasticity (tLTP vs  
351 tLTD) could allow an efficient stabilization of learning and avoid synaptic saturation.

352

### 353 **Acetylcholine**

354 Acetylcholine acts on two types of muscarinic receptors (mAChRs): the M<sub>1</sub>- (M<sub>1</sub>, M<sub>3</sub>  
355 and M<sub>5</sub>) and M<sub>2</sub>- (M<sub>2</sub> and M<sub>4</sub>) class receptors (Thiele, 2013), and the ionotropic (cationic)  
356 nicotinic receptors (nAChRs) (Albuquerque et al., 2009). M<sub>1</sub>-class mAChRs are Gq/G11-  
357 coupled leading to inositol 1,4,5-triphosphate and diacylglycerol production (*via*  
358 phospholipase C $\beta$  activation), subsequent increase of intracellular calcium and activation of  
359 protein kinase C (Fig. 2a); M<sub>2</sub>-class mAChRs are Gi/Go-coupled, leading to inhibition of  
360 adenylate cyclase, and a reduction of cAMP and thus protein kinase A activity.

361 Unlike STDP experiments with noradrenaline and dopamine, experiments to  
362 characterize the effect of acetylcholine have not carefully delineated M<sub>1</sub>-class vs M<sub>2</sub>-class  
363 effects; thus experimental results are more diverse. At hippocampal CA1 pyramidal cells,  
364 bidirectional Hebbian STDP is converted into unidirectional tLTP after enhancement of  
365 acetylcholine (Brzosko et al., 2017) (Fig. 1b), whereas inhibition of mAChRs prevents post-  
366 pre tLTD and converts pre-post tLTP into tLTD (Sugisaki et al., 2011; Sugisaki et al., 2016).  
367 When excitatory and inhibitory post-synaptic currents were examined at synapses of CA1  
368 pyramidal neurons, pre-post pairings induce tLTP of excitatory pathway while it triggers  
369 tLTD at inhibitory pathways via the co-activation of mAChRs and CB<sub>1</sub>R (Ahumada et al.,  
370 2013). Thus, Hebbian STDP in CA1 pyramidal neurons depends on the excitation/inhibition  
371 balance, which is tightly regulated by mAChRs expressed in GABAergic interneurons and  
372 pyramidal cells (Ahumada et al., 2013; Sugisaki et al., 2011; Takkala and Woodin, 2013;  
373 Sugisaki et al., 2016).

374 Though acetylcholine alone seems to promote unidirectional plasticity (tLTP- or  
375 tLTD-only), co-activation of mAChRs and Gs coupled pathways (either D1/D5 dopaminergic  
376 receptors in the hippocampus CA1 pyramidal cells (Brzosko et al., 2017) or  $\beta$ -adrenergic

377 receptors in visual cortex layer 2/3 pyramidal cells (Seol et al., 2007)) promotes bidirectional  
378 plasticity by restoring Hebbian tLTP for  $\Delta t_{\text{STDP}} > 0$  (Fig. 2b).

379 The effects of acetylcholine *via* nAChR-activation are expected to include  
380 depolarization and possibly increased calcium influx (Jones et al., 2012), but they also can  
381 exert a more subtle influence on STDP by regulating the magnitude of STDP rather than its  
382 polarity or expression (Sugisaki et al., 2016). Nicotine increases the threshold for the  
383 induction of Hebbian tLTP at excitatory synapses of pyramidal cells of the prefrontal cortex  
384 (Couey et al., 2007). However, note that nicotine when applied at a high concentration  
385 ( $\sim 10\mu\text{M}$ ) can exert a more drastic effect on STDP since it converts tLTP into tLTD (Couey et  
386 al., 2007). Interestingly, in the medial prefrontal cortex, after nicotine treatment in juvenile  
387 rats, opposing effects are obtained depending on the developmental stage: tLTP magnitude  
388 was reduced in juvenile whereas it was increased in adult rats (Goriounova and Mansvelder,  
389 2012).

390

391 Taken together, the above results reveal a general principle whereby the  
392 neuromodulatory effects exerted on STDP by monoamines (dopamine or noradrenaline) or  
393 acetylcholine are for a large part guided by the type of G-protein activated (regardless of the  
394 agonist): Gi/o-coupled and Gq/11-coupled receptor activation facilitates tLTD ( $D_2$ -class,  $\alpha 1$ -  
395 adrenergic,  $M_1$ -class), whereas Gs- and Golf-coupled receptor activation rather leads to the  
396 expression of tLTP ( $D_1$ R-class,  $\beta$ -adrenergic receptors). However the validity of this general  
397 principle needs further investigation in other brain areas and neuronal subtypes.

398

### 399 **Brain-derived neurotrophic factor (BDNF)**

400 The neurotrophic factor BDNF binds to the tyrosine receptor kinase B, which induces  
401 tyrosine receptor kinase B dimerization and the autophosphorylation of tyrosine residues in  
402 the cytoplasmic kinase domain. This process induces the activation of three main signaling  
403 pathways: phospholipase  $C\gamma$ , phosphoinositide 3-kinase and extracellular signal-regulated  
404 protein kinases cascades. Notably, the phosphoinositide 3-kinase signaling pathway plays an  
405 important role in the regulation of mRNA translation, which impacts protein synthesis and  
406 putatively BDNF-dependent plasticity. Numerous studies have shown the role of BDNF in  
407 modulating synaptic transmission and plasticity (for reviews see Park and Poo, 2013;  
408 Edelman et al., 2014).

409 Concerning STDP, pairings of glutamate release and postsynaptic spiking at 1Hz are  
410 sufficient to release BDNF from the postsynaptic dendrites in a spike-timing-dependent  
411 manner (for  $0 < \Delta t_{\text{STDP}} \leq +20\text{ms}$ ; for  $\Delta t_{\text{STDP}} > 20\text{ms}$  BDNF release was not detected) (Lu et al.,  
412 2014). This spike-timing-dependent BDNF release is dependent on the activation of NMDA  
413 receptors. In hippocampal neurons, the tLTP part of the observed bidirectional Hebbian  
414 STDP depends on BDNF (Bi and Poo, 1998; Lu et al., 2014). Interestingly, depending of the  
415 activity pattern during STDP pairings, the BDNF dependence of the observed plasticity is  
416 different. Indeed, hippocampal tLTP induced with presynaptic activation paired with  
417 postsynaptic bursts of four back-propagating action potentials (1:4 pairings repeated 30 times  
418 at 0.5 Hz) is BDNF and tyrosine receptor kinase B-mediated, whereas canonical STDP  
419 pairings (1:1 pairings repeated 100 times at 0.5 Hz) induced a tyrosine receptor kinase B-  
420 independent tLTP at the same synapses (Edelmann et al., 2015). Genetic impairment of  
421 BDNF synthesis has led to alteration of STDP in the prefrontal cortex. Disruption of one of  
422 the promoters involved in BDNF transcription (promoter IV mutant mice) leads to the  
423 aberrant induction of tLTP, which is absent in wild-type mice, for 50 pairings (Sakata et al.,  
424 2009). In the infralimbic medial prefrontal cortex, STDP is absent in a rodent model (BDNF-  
425 Met/Met mice) of the human BDNF Val66Met polymorphism (leading to severe cognitive  
426 dysfunction and anxiety disorders) in which the BDNF release is impacted; STDP is  
427 recovered after exogenous BDNF application (Pattwell et al., 2012).

428

#### 429 **Nitric oxide (NO)**

430 NO, an intercellular messenger, is generated by the enzyme NO synthase and activates  
431 soluble guanylyl cyclase leading to cGMP formation. In turn, cGMP-activated protein  
432 kinases regulate multiple substrates such as DARPP-32 and G-substrate, which inhibits  
433 phosphatases that are involved, among other effects, in synaptic plasticity expression (for  
434 review see: Hardingham et al., 2013). Concerning STDP, in the somatosensory cortex of  
435 mice, Hebbian tLTP depends both on the AMPAR-subunit-1 and a NO-dependent  
436 presynaptic component (Hardingham and Fox, 2006). Similarly, glutamate afferents to  
437 serotonergic neurons of the dorsal raphe nucleus exhibit tLTP for pre-post pairings, which  
438 is NO-dependent, involving the cGMP-activated protein kinase signaling cascade (Haj-  
439 Dahmane et al., 2017). In retinal ganglion cells of tadpoles, STDP can be induced by natural  
440 visual stimulation (*e.g.* moving bar) or by electrical stimulation of the retina and in both  
441 cases, NO is required for tLTD while BDNF is required for tLTP (Mu and Poo, 2006).

442

### 443 **GABA**

444 In the dorsal striatum, anti-Hebbian STDP as observed in control conditions in striatal output  
445 neurons is shifted to Hebbian STDP under pharmacological blockade of GABA<sub>A</sub>R receptors  
446 (Fino et al., 2010; Paillé et al., 2013; Valtcheva et al., 2017) (Fig. 3a). This effect applies  
447 equally at D<sub>1</sub>R-class striatopallidal (direct pathway) and D<sub>2</sub>R-class striatonigral (indirect  
448 pathway) neurons of juvenile and adult rodents. Although the molecular mechanisms  
449 underneath this reversal of polarity by GABA are not fully elucidated, a computational model  
450 suggests that depolarizing effects of GABA at distal dendrites would reverse calcium influx  
451 by modifying the balance between calcium influxes from NMDAR *vs* voltage-sensitive  
452 calcium channels (Paillé et al. 2013). Although GABA increases calcium influxes in both  
453 NMDAR and voltage-sensitive calcium channels, *via* its depolarizing effect in striatal output  
454 neurons (due to the relative values of the chloride reversal and membrane potential), the  
455 depolarizing effect of GABA would impact differentially NMDAR and voltage-sensitive  
456 calcium channels depending on the order of pairings (post-pre *vs* pre-post). GABA would  
457 favor calcium influx via voltage-sensitive calcium channels for post-pre pairings (promoting  
458 tLTP), whereas it would favor calcium influx via NMDARs for pre-post pairings (promoting  
459 tLTD) in control conditions, leading to anti-Hebbian STDP (Paillé et al., 2013). Under  
460 GABA blockade, this balance between calcium influxes is shifted and Hebbian STDP can be  
461 observed. Change in GABAergic signaling during striatal development (*i.e.* the onset of the  
462 tonic GABAergic signaling around P<sub>14</sub>; Ade et al., 2008) appears to be a key factor for  
463 shaping of striatal STDP. Indeed, in young rats (P<sub>7-10</sub>) corticostriatal STDP is unidirectional  
464 and Hebbian (tLTD with post-pre pairings, no plasticity with pre-post pairings) but  
465 bidirectional and anti-Hebbian in adult rodents (Valtcheva et al., 2017) (Fig. 3a). GABA  
466 signaling is also at play with the control of CB<sub>1</sub>R-dependent tLTP which expression shifts  
467 from post-pre to pre-post stimulation when ionotropic GABA<sub>A</sub> transmission is blocked (Cui  
468 et al., 2015). GABA is not involved in the induction of STDP *per se*, nor its magnitude, but  
469 controls STDP polarity, *i.e.* the association between the sign of the pairing (pre-post or post-  
470 pre) and the plasticity outcome (tLTP or tLTD). The tonic GABAergic component plays a  
471 major role in the emergence of the anti-Hebbian striatal STDP in juvenile and adult rodents  
472 (Valtcheva et al., 2017) (Fig. 3a). Thus, the pathological deregulation of tonic GABAergic  
473 signaling may affect the polarity and occurrence of striatal plasticity and alter procedural

474 learning and memory. It remains to be seen whether the neuromodulator role of GABA for  
475 STDP emergence and/or polarity constitutes a general rule in the brain.

476 Change of STDP polarity induced by GABAergic transmission has also been observed in  
477 hippocampus. In hippocampal CA1 pyramidal cells, blockade of GABA<sub>A</sub>Rs converts  
478 unidirectional tLTD to bidirectional Hebbian STDP (with 80 pairings at 5Hz) (Sugisaki et al.,  
479 2016) (Fig. 3b). The modulatory effects of GABA<sub>A</sub> and GABA<sub>B</sub> receptors can also combine.  
480 Indeed, at Schaffer collateral-CA1 excitatory synapses of the rat hippocampus, plasticity  
481 relies on postsynaptic GABA<sub>A</sub> receptors to set the spike-timing dependency and also depends  
482 on presynaptic GABA<sub>B</sub> receptors for its frequency dependence (Nishiyama et al., 2010) (Fig.  
483 3b). Specifically, postsynaptic GABA<sub>A</sub> receptors regulate the timing dependence of tLTD at  
484 5Hz pairings (in the theta frequency band), whereas presynaptic GABA<sub>B</sub> receptors control the  
485 frequency dependence of tLTD at 25Hz (alpha and beta frequencies) and also accounts for  
486 the expression of tLTP for 5Hz and 50Hz (gamma frequencies) (Nishiyama et al., 2010). In  
487 addition, STDP can be expressed at GABAergic interneurons, where it modulates the strength  
488 of GABAergic inhibition since STDP pairings alters the activity of potassium-chloride  
489 cotransporter-2, resulting in changes in the reversal potential of GABAergic synaptic currents  
490 (Woodin et al., 2003).

491

492 Taken together, the above results indicate that the spectrum of the third factor of STDP is  
493 very large since in addition to neuromodulators it can be extended to BDNF, NO and  
494 neurotransmitters acting as neuromodulators such as GABA. STDP synaptic plasticity is thus  
495 modulated, whether in its induction, its direction or its temporal window. Though  
496 neuromodulation of STDP has been investigated for the early phase of plasticity (within the  
497 first hour, *i.e.* the induction phase), the effects of neuromodulators remain to be investigated  
498 for the late phases of plasticity in which the third factor is expected to have a crucial role for  
499 the maintenance of memory (Lisman et al., 2011).

500

### 501 **Modulation of STDP by astrocytes: the forgotten third factor**

502 Many forms of excitatory STDP rely on either pre- or postsynaptic glutamate  
503 receptors (Sjöström et al., 2008; Feldman, 2012; Korte and Schmitz, 2016). Therefore, STDP  
504 is expected to be tightly controlled by glutamate dynamics. Specifically, the spatiotemporal

505 profile of glutamate may define the extent and location of recruited glutamate receptors,  
506 which are involved in the induction of tLTP or tLTD.

507 An overriding question is how coincident synaptic activity in the millisecond range  
508 can be integrated over a longer timescale during the iteration of pre- and postsynaptic  
509 pairings to allow STDP induction, while keeping sharp sensitivity to timing during individual  
510 pairing episodes. A potential solution to this problem could be that (1) glutamate should be  
511 released in a delayed manner to allow integration of pre- and postsynaptic activity over the  
512 time course of minutes; and (2) synaptically released glutamate during neuronal activity  
513 needs to be reliably cleared from the extracellular space to allow high fidelity sampling of  
514 coincident pre- and postsynaptic activity during STDP pairings. Astrocytes help solve this  
515 problem of controlling extracellular glutamate dynamics and have been shown to play an  
516 important role in synaptic transmission, as well as short- and long-term memory (Chung et  
517 al., 2015; Oliveira et al., 2015). This role of astrocytes has led to the concept of the tripartite  
518 synapse, comprised of the pre- and postsynaptic neuronal elements as well as the astrocytes.  
519 Indeed, a substantial part of central synapses are contacted by astrocytes (Bernardinelli et al.,  
520 2014). Notably, astrocytes are able to release glutamate *via* exocytosis in response to  
521 neuronal activity (Araque et al., 2014; Sahlender et al., 2014; Verkhratsky et al., 2016) and to  
522 efficiently clear glutamate from the extracellular space on a submillisecond timescale *via*  
523 high-affinity glutamate transporters (Danbolt, 2001). Therefore, astrocytes can both detect  
524 and control neuronal activity *via* the release and reuptake of glutamate.

525 Astrocytes can integrate the coincident neuronal activity during STDP pairings and  
526 participate in the induction of tLTD (Min and Nevian, 2012). Excitatory tLTD induced by  
527 post-pre pairings at layer 4 onto layer 2/3 synapses in the rat barrel cortex relies on the  
528 release of endocannabinoids by the postsynaptic element through the activation of astrocytic  
529 CB<sub>1</sub>Rs. In turn, glutamate released by astrocytes activates presynaptic NMDARs which are  
530 required for tLTD induction (Rodríguez-Moreno and Paulsen, 2008). Astrocytes are able to  
531 sense postsynaptic endocannabinoid release by gradually increasing their calcium waves  
532 exclusively during repetitive post-pre pairings within a narrow temporal window of  $\Delta t_{\text{STDP}} = -$   
533 25 ms which is eligible for tLTD induction. Indeed, pre-post pairings at  $\Delta t_{\text{STDP}} = +25$  ms and  
534 post-pre pairings at  $\Delta t_{\text{STDP}} = -250$  ms, which induce tLTP and no plasticity, respectively, do  
535 not trigger any changes in calcium dynamics. Therefore, astrocytes are selective to a unique  
536 temporal pattern, which both generates calcium dynamics to promote glutamate release and  
537 imposes a threshold for tLTD induction. Astrocytes can thus act as a time buffer by

538 integrating coincident pre- and postsynaptic activity over the time course of minutes and  
539 enabling tLTD by delayed release of glutamate.

540         Astrocytes also are crucial for the gating of both tLTP and tLTD in the dorsal striatum  
541 *via* the uptake of glutamate (Valtcheva and Venance, 2016). Physiological activity of the  
542 astrocytic glutamate transporter, called the excitatory amino acid transporter-2 (EAAT2),  
543 allows the expression of bidirectional anti-Hebbian STDP induced in a narrow temporal  
544 window  $-30 < \Delta t_{\text{STDP}} < +30$  ms (Fino et al., 2010; Paillé et al., 2013; Valtcheva and Venance,  
545 2016). When EAAT2 is blocked, a form of LTP that does not rely on coincident detection can  
546 be induced by uncorrelated activation of pre- and postsynaptic elements. This non-Hebbian  
547 LTP requires postsynaptic back-propagating action potentials and extrasynaptic GluN2B-  
548 containing NMDARs, which are activated by glutamate spillover. In contrast, the  
549 overexpression of EAAT2 prevents the expression of striatal STDP (Valtcheva and Venance,  
550 2016) possibly by restricting glutamate availability for both the NMDARs and mGluRs  
551 required for striatal STDP (Fino et al., 2010; Shen et al., 2008). Thus, preserving the optimal  
552 temporal contingency between pre- and postsynaptic activity required for STDP depends on  
553 astrocytic glutamate uptake. Astrocytes gate tLTP and tLTD by a subtle regulation of the  
554 extracellular glutamate levels and, therefore, a precisely tuned range of EAAT2 activity  
555 allows the emergence of STDP. Computational models have begun to explore interactions  
556 between glutamatergic synapses and astrocytes (De Pitta et al, 2011; De Pitta and Brunel  
557 2016; see also De Pitta et al 2012 for a review), but investigating the role of astrocytic  
558 glutamate control requires transforming the binary glutamate release event typically used in  
559 STPD models into glutamate diffusion and uptake mechanisms.

560         Astrocytes can release various other neurotransmitters and factors besides glutamate  
561 (Araque et al., 2014; Sahlender et al., 2014; Verkhratsky et al., 2016) including the NMDAR  
562 co-agonist D-serine which regulates different forms of synaptic plasticity. The release of D-  
563 serine is necessary for frequency-dependent LTD and LTP in the hippocampus (Henneberger  
564 et al., 2010; Zhang et al., 2008) and prefrontal cortex (Fossat et al., 2011). Moreover,  
565 experience-dependent changes in the degree of synaptic enwrapment by astrocytes governs  
566 the level of D-serine availability and subsequently controls the expression of NMDAR-  
567 dependent LTP and LTD in the supraoptic nucleus of the hypothalamus of lactating rats  
568 (Panatier et al., 2006). The NMDARs implicated in STDP can be situated at both pre- or  
569 postsynaptic sites (Feldman, 2012; Korte and Schmitz, 2016) and thus may be affected to  
570 different extents by gliotransmission. D-serine has a permissive role for the induction of

571 NMDAR-dependent tLTP at mossy fiber-CA1 hippocampal synapses (Rebola et al., 2011),  
572 although its glial origin has not been investigated. In the developing hippocampus a  
573 presynaptic tLTD at CA3-CA1 synapses requires D-serine signaling possibly released from  
574 astrocytes (Andrade-Talavera et al., 2016). Interestingly, the same STDP pairing protocol  
575 induces tLTP at later developmental stages suggesting the possibility that astrocytic coverage  
576 of neurons and modulation of STDP by gliotransmission may be developmentally regulated.

577 Another important gliotransmitter is ATP, which is enzymatically converted to  
578 adenosine in the extracellular space and can act on pre- and postsynaptic adenosine receptors  
579 situated on neurons. Glial release of ATP controls the magnitude of hippocampal LTP  
580 induced with high-frequency stimulation (Pascual et al., 2005) and blockade of postsynaptic  
581 adenosine A2a receptor increases the amplitude of low-frequency stimulation-dependent  
582 LTD in the striatum (Lerner et al., 2010). Adenosine also mediates striatal tLTP *via*  
583 postsynaptic adenosine A2a receptors both *in vitro* (Shen et al., 2008) and *in vivo* when the  
584 STDP paradigm is coupled with dopamine pairing (Fisher et al., 2017). In addition,  
585 presynaptic adenosine A1 receptors modulate the amplitude of tLTP in the visual cortex  
586 (Bannon et al., 2017). However, evidence directly implicating astrocytes in the purinergic  
587 control of STDP is still lacking. Computational models of signaling pathways underlying  
588 STDP have begun to include adenosine A2a receptors (see below), but investigation of  
589 interaction between pre-synaptic NMDA and adenosine A1 receptors requires modeling of  
590 mechanisms controlling pre-synaptic vesicle release.

591 Finally, astrocytes are involved in the GABAergic modulation of both the polarity  
592 (Fino et al., 2010; Paillé et al., 2013; Valtcheva et al., 2017) and threshold for induction  
593 (Groen et al., 2014) of excitatory STDP. Astrocytes regulate basal and transient inhibitory  
594 tone *via* GABAergic transporters (Scimemi, 2014). Non-specific blockade of both neuronal  
595 and astrocytic GABA transporters in the developing striatum has a permissive role for the  
596 induction of tLTD (Valtcheva et al., 2017) but the particular contribution of astrocytic GABA  
597 clearance in STDP remains to be explored.

598

## 599 **MOLECULAR PATHWAY-BASED COMPUTATIONAL MODELS OF STDP**

600 In an attempt to better understand the mechanisms governing learning and memory  
601 and determine which mechanisms control input-dependent plasticity, modeling efforts have  
602 focused on biophysical and biochemical models that utilize a kinetic description of the

603 molecular pathways implicated in STDP. These models range in molecular complexity from  
604 single ion (*i.e.* calcium) to complicated signaling pathways, and in spatial complexity from  
605 single-compartment (Fig. 4a1) to multi-compartment (Fig. 4a2). An overview of this  
606 literature can be found in several review articles (see *e.g.* Graupner and Brunel, 2010; Griffith  
607 et al., 2015). In the following, we focus on the articles published after 2010, though include  
608 the most influential contributions published before that date. Moreover, in the following, we  
609 subdivide the models into two types: those evaluating the control of plasticity from calcium  
610 dynamics alone, and those that add one or more downstream signaling pathway molecules. In  
611 addition, we try to distinguish single-compartment models from those that add some degree  
612 of spatial structure to the postsynaptic neuron. We acknowledge that in both of these  
613 dimensions the classification is not binary and some models bridge the divide.

#### 614 **Simplified calcium dynamics and two-threshold rules**

615 Models of calcium dynamics in response to STDP stimuli are the most common type  
616 of models, and are justified both by the critical role of calcium in plasticity and also by the  
617 stimulation protocol in which neuromodulator release does not change. The only difference  
618 between STDP protocols that produce tLTP and STDP protocols that produce tLTD is the  
619 timing between the presynaptic stimulation and the postsynaptic action potential,  $\Delta t_{\text{STDP}}$ ; thus  
620 the number and frequency of presynaptic stimulations does not differ between tLTP and  
621 tLTD. This implies that presynaptic release of neuromodulators does not differ so it must be  
622 postsynaptic molecules activated by calcium dynamics that determine the polarity of  
623 plasticity.

624 Calcium predicting the direction of synaptic plasticity is one of the ideas that are  
625 popular among theoreticians and experimentalists. In the simplest form the peak calcium (or  
626 indeed the amplitude of the current through the calcium permeable, NMDA subtype of the  
627 glutamate receptor) controls the direction of plasticity (for reviews see: Evans and Blackwell  
628 2015; Graupner and Brunel, 2010; Griffith et al., 2015). This is known as the “two-threshold”  
629 rule: if calcium (either peak or integrated) is above the higher, potentiation threshold, tLTP is  
630 induced, whereas if calcium is larger than the lower LTD threshold but lower than the LTP  
631 threshold, tLTD occurs (Fig. 4c1). Pre-post pairings produce a large calcium influx through  
632 the NMDA receptor channel with calcium concentration above the LTP threshold, whereas  
633 post-pre pairings produce a moderate calcium influx with calcium concentration between the  
634 LTD and LTP thresholds. One of the first models of NMDAR-dependent synaptic plasticity  
635 was proposed by Shouval et al. (2002). This model, using simplified calcium dynamics inside

636 a dendritic spine, accounted for a diverse range of stimulation protocols such as STDP and  
637 classical rate-based plasticity; however it predicted depression for long positive  $\Delta t_{\text{STDP}}$ , a  
638 model prediction which is not confirmed by experiments (but see Nishiyama et al., 2000;  
639 Wittenberg and Wang, 2006; Nishiyama et al., 2010). In the dorsal striatum, a model of  
640 calcium dynamics (Evans et al. 2012) evaluated the role of NMDAR subunit (2A and 2B  
641 subunits) in shaping the sensitivity to timing dependence, and correctly predicted that  
642 NMDAR-2A would require a small  $\Delta t_{\text{STDP}}$ , whereas NMDAR-2B can support tLTP with a  
643 large  $\Delta t_{\text{STDP}}$ . Several extensions or modifications to the basic model have been made both to  
644 account for results with spike triplets (*i.e.*, when either two presynaptic stimuli or two  
645 postsynaptic action potentials are generated) and to minimize the tLTD window for long  
646 positive spike-timings. Adding another coincidence detection of presynaptic NMDA  
647 receptors with endocannabinoids is one mechanism utilized in a neuromorphic  
648 implementation of calcium based synaptic plasticity (Rachmuth et al., 2011). Alternatively,  
649 incorporating short term depression of transmitter release or AP back-propagation (Shouval  
650 and Kalantzis, 2005, Bush and Jin, 2012) minimizes the tLTD seen with long positive  $\Delta t_{\text{STDP}}$   
651 and can account for other experimental results; however, a more broadly applicable study  
652 (Rubin et al. 2005) showed that plasticity rules that use calcium amplitude alone cannot  
653 completely avoid predicting tLTD for long positive timings.

654 An extension of the two-threshold rule states that the duration of calcium elevation is  
655 equally important in determining direction of plasticity (Fig. 4c2). Several models of STDP  
656 explicitly take into account both the amplitude and the duration of calcium in predicting  
657 plasticity outcome (Kumar and Mehta, 2011; Graupner and Brunel, 2012). Including a  
658 duration threshold or integrating the total calcium response allows correctly predicting  
659 experimental outcomes for both traditional STDP curves and STDP curves produced by spike  
660 triplets. Another extension of the Shouval et al., (2002) model, Standage et al. (2014),  
661 implements a calcium-dependent, sigmoid-shaped time constant of calcium decay, which  
662 represents saturation of calcium extrusion from the spines. This model shows that saturation  
663 of calcium extrusion might be responsible for the dependence of tLTP on the (theta-  
664 frequency like) inter-spike interval for triplet stimulation protocols. Including the duration of  
665 calcium does not exclude consideration of presynaptic release probability on STDP. Indeed,  
666 gliotransmission may change the shape of the STDP curve depending on whether  
667 gliotransmitters increase or decrease presynaptic release (De Pitta and Brunel 2016).

668 **Threshold rules based on detailed calcium dynamics**

669 Most of the aforementioned models use simplified calcium dynamics instead of  
670 explicitly implementing the mechanisms underlying control of calcium (Fig. 4b), which  
671 might improve predictions of synaptic plasticity. In other words, the next set of models used  
672 neither single time constant of decay nor summation of independent pre- and postsynaptic  
673 components for calcium dynamics. Though not explicitly implementing a STDP rule, Griffith  
674 et al., (2016) indirectly consider the effect of calcium duration by using calcium-bound  
675 calmodulin to assess how back-propagating action potential timing influences calcium  
676 concentration. Using a 3-dimensional, deterministic reaction-diffusion model of calcium  
677 interactions with calmodulin and other calcium binding proteins within a dendritic spine,  
678 Griffith et al. (2016) show that calcium-bound calmodulin is a more sensitive indicator of  
679 spike timing than free calcium. They further demonstrate the role of neuromodulators in  
680 regulating synaptic plasticity through their activation or inhibition of calcium dependent  
681 potassium channels during an STDP protocol, which greatly modulates calmodulin  
682 activation.

683 Several studies explicitly investigate how the dendritic location and inhibitory inputs  
684 shape the local calcium-based plasticity rules (Bar-Ilan et al., 2013; Jędrzejewska-Szmek et  
685 al. 2016). Bar-Ilan et al. (2013) showed that inhibition shapes the spatial profile of dendritic  
686 calcium concentration in neocortical pyramidal neurons. Depending on the location of the  
687 excitatory and inhibitory inputs on the dendritic tree (Fig. 4a2), tLTP may be blocked,  
688 transformed to tLTD, or the synapse may undergo no plasticity. Similarly, Jędrzejewska-  
689 Szmek et al. (2016) developed a computational model of the major neuron type in the  
690 striatum, the striatal output neurons, including both electrical activity and calcium dynamics.  
691 They demonstrated that calcium amplitude and duration together (Fig. 4c2) can predict a  
692 wide range of experimental plasticity outcomes, and further demonstrated a distance  
693 dependence of STDP caused by the back-propagating action potential. In both of these  
694 models, the distance dependent decreases in back-propagating action potential amplitude  
695 reduces calcium influx through NMDA receptors for more distant synapses. This reduced  
696 calcium influx can convert tLTP into either tLTD or no plasticity. These publications  
697 demonstrate that by modeling mechanisms controlling calcium dynamics, including  
698 diffusion, buffers and pumps, and by considering calcium duration, the LTD window for long  
699 positive  $\Delta_{\text{STDP}}$  is avoided.

700 An aspect of calcium dynamics often ignored in modeling studies is calcium release  
701 from intracellular stores. This has been shown to contribute to tLTP under some conditions

702 (Plotkin et al., 2013; Cui et al, 2016). Thus, Nakano et al., (2013) included calcium release  
703 from stores in their multi-compartmental model of a direct pathway spiny projection neuron.  
704 In addition, though not explicitly including other signaling pathways, they evaluated the  
705 effect of dopaminergic modulation of calcium, potassium and NMDAR channels. The main  
706 result of their simulations showed that dopaminergic input preceding a back-propagating  
707 action potential induced higher calcium responses than dopamine input following a back-  
708 propagating action potential. This study also predicted that the timing dependence of calcium  
709 responses between the up- and down-states was similar.

### 710 **Models of signaling pathway to explain synaptic plasticity**

711 Beyond calcium, several models add on simplified or abstract version of downstream  
712 signaling molecules. Rubin et al., 2005 propose a three detector system, loosely based on  
713 pathways resembling the opposing CaMKII – protein phosphatase signaling pathways. In  
714 brief, three calcium-sensitive detectors are implemented: high, transient calcium levels  
715 activate the tLTP detector; low calcium elevations activate the tLTD detector; and  
716 intermediate calcium levels activate a “Veto” detector. Another variable integrates both the  
717 tLTD detector and the Veto detector (called a double filter), such that intermediate calcium  
718 levels decrease the double filter value; thus the double filter detects the uninterrupted  
719 duration of calcium at low values yet suppresses the development of tLTD should calcium  
720 spend some time at intermediate values, such as occurs with long positive  $\Delta t_{\text{STDP}}$ . Using the  
721 three calcium detector system of Rubin et al. (2005), Cutsuridis (2011) showed that single  
722 GABAergic inhibitory inputs can sharpen the shape of the STDP curve: narrowing the  
723 temporal window that supports tLTD, whereas a train of GABAergic inputs both sharpens the  
724 tLTD window and reduces the tLTP amplitude. A follow-up study (Cutsuridis, 2012)  
725 extended the model to burst stimulation, and predicted that GABAergic inputs would expose  
726 a tLTD window for long positive  $\Delta t_{\text{STDP}}$ . The timing of the GABA inputs determined whether  
727 the effect was predominantly depression or potentiation.

728 Several models (Graupner and Brunel, 2007; Carlson and Giordano, 2011; Graupner  
729 and Brunel, 2012; Mihalas, 2012; Saurdargiene and Graham, 2015; Pi and Lisman, 2008; Cui  
730 et al, 2016; for reviews see: Graupner and Brunel, 2010; Evans and Blackwell, 2015; Griffith  
731 et al., 2015) have implemented even more realistic representations of signaling pathway  
732 kinetics, including the calcium activated phosphatase calcineurin, the calcium activated  
733 kinase, CaMKII, and the Gs-activated adenylyl cyclase, the latter of which produces cAMP to  
734 activate protein kinase A (Fig. 5). Additional pathways, such as protein kinase C (resulting

735 from activation of Gq-coupled receptors such as M<sub>1</sub>R and mGluR) and ERK (downstream of  
736 protein kinases A, C and tyrosine receptor kinase B) are also involved. Several advantages  
737 accrue from these models, including the ability to produce experimentally testable predictions  
738 regarding the role of specific molecules. Another key advantage of simulating signaling  
739 molecules is that the tLTD window for long positive  $\Delta t_{\text{STDP}}$  is eliminated without arbitrarily  
740 assuming the existence of a dedicated calcium concentration range that does not elicit  
741 synaptic plasticity, *i.e.*, a separate range between the tLTD-inducing calcium range and the  
742 tLTP range. Again these models vary in complexity, such as the number of different signaling  
743 pathways included, and whether spatial aspects are included. Several models of these  
744 signaling molecules have been applied to STDP protocols in the cortex, hippocampus and  
745 striatum.

746 One of the earliest models, the single-compartment electric model of Graupner and  
747 Brunel, (2007), couples membrane potential with a biochemical reaction model *via* calcium  
748 dynamics. Phosphorylation state of CaMKII serves as the models readout, *i.e.* the level of  
749 phosphorylated CaMKII serves as a proxy of the synaptic weight. Short positive intervals can  
750 switch the CaMKII to a highly phosphorylated state; whereas negative intervals (but not long  
751 positive intervals) switch the CaMKII to a low phosphorylated state. Critical to success of  
752 this model is adjustment of calcium dependence of protein kinase A and calcineurin activity  
753 against inhibitor 1, which controls the level of free protein phosphatase 1. A high-level of  
754 protein phosphatase 1 will dephosphorylate CaMKII to prevent its persistent activation.  
755 Indeed, in this model (Fig. 5): (i) the protein phosphatase-1/CaMKII activation ratio dictates  
756 plasticity; LTD is expressed when protein phosphatase-1 activation overcomes CaMKII,  
757 whereas LTP occurs when CaMKII activation is larger than protein phosphatase-1 activation,  
758 and (ii) protein phosphatase-1 activity is maximal at intermediate calcium levels whereas  
759 CaMKII activation needs larger calcium levels. Short negative  $\Delta t_{\text{STDP}}$  yield intermediate but  
760 long lasting calcium levels, which efficiently activate protein phosphatase-1 but are not large  
761 enough to activate CaMKII, thus triggering LTD. Short positive  $\Delta t_{\text{STDP}}$  yield sharp calcium  
762 peaks that are large enough to activate CaMKII but do not persist long enough around  
763 intermediate values to activate protein phosphatase-1 significantly; this leads to LTP. Finally,  
764 the calcium levels triggered by long positive  $\Delta t_{\text{STDP}}$  are too weak to activate CaMKII but do  
765 not stay long enough around intermediate values to activate protein phosphatase-1. Long  
766 positive  $\Delta t_{\text{STDP}}$  therefore fail to activate either the protein phosphatase-1 or CaMKII, which in  
767 effect rules out the expression of tLTD. This molecular system therefore exhibits dynamics

768 similar to the "Veto" detector proposed by Rubin et al. (2005) to eliminate tLTD at long  
769 positive spike timings (see above).

770 Subsequent models either enhance the electrical activity model, or add AMPA  
771 receptors as a model readout. Urakubo et al. (2008) develop a multi-compartment, multi-ion  
772 channel model of visual cortex pyramidal neurons to activate a biochemical reaction model.  
773 In contrast to Graupner and Brunel (2007), the timing dependence of tLTD cannot be  
774 reproduced unless calcium-bound calmodulin allosterically inhibits NMDARs. Both Carlson  
775 and Giordano (2011) and Saurdargiene and Graham (2015) used a model of AMPAR  
776 insertion controlled by the CaMKII/protein phosphatase-2A switch. Carlson and Giordano  
777 (2011) used a single-compartment model of calcium dynamics (from Shouval et al. 2002) to  
778 activate the biochemical network model of Pi and Lisman, (2008). This single-compartment  
779 model can explain STDP and does not predict tLTD for long positive  $\Delta t_{\text{STDP}}$ . Voltage-  
780 sensitive calcium channels are critical for the latter effect, as blocking voltage-sensitive  
781 calcium channels allow tLTD to emerge for long positive  $\Delta t_{\text{STDP}}$ . Saudargiene and Graham  
782 (2015) incorporated spatial aspects of calcium dynamics by using a detailed compartmental  
783 model of pyramidal CA1 neuron (Poirazi et al, 2003) to activate a biochemical network  
784 model derived from two earlier models (Pi and Lisman, 2008; Graupner and Brunel, 2007).  
785 Saudargiene and Graham (2015) showed, by monitoring AMPAR phosphorylation by the  
786 CaMKII/protein phosphatase-2A switch, that tLTD is indeed induced by lower calcium levels  
787 than tLTP, and that tLTD also requires many more repetitions of this lower calcium (which is  
788 consistent with experimental results). Saudargiene and Graham (2015) also investigated the  
789 influence of particular timings of inhibition associated with excitatory inputs, showing that  
790 inhibition affects tLTD more than tLTP, because tLTD occurs for moderate calcium levels  
791 and is thus more vulnerable to any reduction in peak calcium.

792 Whereas spatial models of calcium dynamics typically include dendritic branching or  
793 explicit spines (microdomains), many signaling molecules are anchored *via* structural  
794 proteins into multi-protein complexes, effectively creating nanodomains of molecule  
795 interactions. One method for evaluating the effect of nanodomains (without explicitly  
796 creating a spatial model) is to couple different sources of calcium to different downstream  
797 signaling molecules. This approach was utilized by Mihalas (2011) who coupled three  
798 different calcium sources to three different signaling molecules: NMDAR to CaMKII,  
799 voltage-sensitive calcium channels to calcineurin, and phosphodiesterase to calcium release.  
800 Adenylyl cyclase was coupled to both voltage-sensitive calcium channels and NMDAR. The

801 change in synaptic weight was calculated from kinase (tLTP) and phosphatase (tLTD)  
802 activity. This model investigated the role of cAMP degradation in triplet-based STDP, and  
803 showed that, if cAMP activity is spatially restricted to the membrane, the STDP profile is  
804 similar to that observed in cortical layer 2/3 slices. The STDP profile for spatially diffuse  
805 cAMP activity was consistent with that observed in hippocampal cell culture.

806 In the striatum, endocannabinoid production and activation of CB<sub>1</sub>Rs are required for  
807 most forms of tLTD (Mathur and Lovinger, 2012); thus, Cui et al. (2016) extended the  
808 signaling pathways from Graupner and Brunel (2007) with 2-arachidonoylglycerol (the main  
809 endocannabinoid) production via mGluR- and M<sub>1</sub>R activation. Cui et al. (2016) utilized a  
810 single-compartment model of electrical activity of a spiny projection neuron for calcium  
811 dynamics, coupled with a model of signaling pathways underlying STDP in striatum,  
812 including calcium-induced calcium release from internal stores. This model used a combined  
813 2-arachidonoylglycerol- and CaMKII-based plasticity rule, where the direction of plasticity  
814 (LTP or LTD) was determined by the product of the presynaptic weight (2-  
815 arachidonoylglycerol-based) and postsynaptic weight (CaMKII based). The strength of this  
816 model is the ability to show the mechanism whereby decreasing the number of pairings  
817 converts NMDAR-dependent tLTP to an endocannabinoid-dependent tLTP, which was  
818 confirmed experimentally (Fig. 5) (Cui et al., 2015; Cui et al., 2016). The underlying  
819 hypothesis of this model (that was confirmed experimentally) is that moderate activation of  
820 CB<sub>1</sub>R caused endocannabinoid-mediated tLTD whereas large CB<sub>1</sub>R activation leads to tLTP.  
821 In the model, 10-20 negative pairings trigger large endocannabinoid transients that result in  
822 endocannabinoid-mediated tLTP. However, CB<sub>1</sub>R desensitization and partial depletion of  
823 calcium in the endoplasmic reticulum starts to be significant after 20 pairings, so that CB<sub>1</sub>R  
824 activation is in fact smaller with more than 20 pairings than with 10-20 pairings. As a result,  
825 the expression of endocannabinoid-mediated tLTP is restricted to 10-20 negative pairings, in  
826 agreement with experimental observations (Cui et al., 2015; Cui et al., 2016). On the other  
827 hand, as in the original model by Graupner and Brunel (2007), calcium levels become large  
828 enough to activate significant amounts of CaMKII only after 40-50 negative pairings, thus  
829 restricting the expression of NMDAR-dependent tLTP to this range of pairings. As a result,  
830 this model successfully reproduces the experimental observation that the endocannabinoid-  
831 mediated tLTP expressed at 10-20 positive pairings disappears, to be replaced by NMDAR-  
832 dependent tLTP after 50 pairings (Fig.5). The addition of presynaptic dopamine signaling to

833 the model correctly predicted that the CB<sub>1</sub>R-dependent tLTP observed with 10-20 pairings is  
834 also under the control of presynaptic D<sub>2</sub>R (Fig. 5).

835

### 836 **Exploring *in vivo*-like conditions**

837 One benefit of computational modeling is the ability to isolate a specific aspect of  
838 STDP and address the impact of this very aspect at the level of networks and/or learning *in*  
839 *vivo*. For instance, Kempter et al., (1998) used spike-based models to explore how the pulse  
840 structure of neuronal signals and events on a millisecond scale influenced learning rules.  
841 Clopath et al. (2010) utilized a voltage-based plasticity rule, consistent with a wide body of  
842 experimental data, to study the emergence from plasticity of connectivity patterns in a  
843 cortical network. Along the same line, variants of the classical computational STDP rule have  
844 been devised that yield broad synaptic weight distributions matching the available  
845 experimental observations (Gilson and Fukai, 2011).

846 However, one major detractor of STDP is its deterministic and constant spike timing  
847 (interval between spikes within a pairing) and inter-stimulation interval (interval between  
848 consecutive pairings), which diverge highly from biological variability. One of the most  
849 pressing questions of learning and memory is which stimuli resemble *in vivo*-like conditions  
850 best. Gjorgjieva et al. (2011) showed that a triplet model of STDP, depending on the  
851 interactions of three precisely timed spikes, described plasticity experiments closer to natural  
852 stimuli measured in the brain. Graupner et al., (2016) compared *in silico* plasticity outcomes  
853 to several types of irregular, *in vivo*-like, firing patterns to investigate the influence of firing  
854 rate and spike timing on synaptic plasticity. They showed that sensitivity of plasticity to  
855 spike-timing is reduced by adding jitter (irregularity) to spike-pairs. Using physiological  
856 firing patterns recorded in awake behaving macaque monkeys, Graupner et al, (2016) further  
857 showed that moderate variation of firing rate, without any timing constraints, could reproduce  
858 synaptic changes induced by spike timing. This result offers a different view on the central  
859 role played by spike timing in long-term synaptic plasticity.

860 Most computational models of STDP indicate that plasticity disappears when the  
861 timing between pre and postsynaptic pairings loses its regularity. However, it is not clear  
862 what amount of noise can be tolerated for STDP or ITDP to be expressed (robustness) and  
863 whether this amount depends on the signaling pathway supporting the plasticity. This  
864 question has recently been tackled both experimentally and in a computational model, using

865 noisy STDP stimulations where the timing between the pre- and the postsynaptic stimulations  
866 was jittered (Cui et al. 2018). As stated above, in striatum three forms of STDP are observed:  
867 NMDAR-tLTP, endocannabinoid-tLTD and endocannabinoid-tLTP (Cui et al., 2015; 2016).  
868 These three forms do not show similar sensitivity to jittered spike timing: NMDAR-tLTP  
869 appeared poorly resistant whereas endocannabinoid-plasticity (tLTD and tLTP) appeared  
870 more robust (Cui et al. 2018). Moreover, increasing the average pairing frequency or the  
871 number of pairings reinforces NMDAR-tLTP and increases resistance to jittered spike timing.  
872 These results suggest that the probability to observe the various forms of STDP *in vivo* is a  
873 multivariate function of the mean spike timing, the number of pairings, the frequency of  
874 pairings and also the variability of the spike timing. The shape of this multivariate function is  
875 thus more complex than *e.g.* a monotonic decay with increasing variability of the spike  
876 timing, and could reveal a functional specialization of each of these STDP forms to sub-  
877 regions of the stimulation train parameters.

878

## 879 **Conclusions and future directions**

880 In addition to the pre- and postsynaptic firing patterns, a third factor for STDP control  
881 comprises not only the classical neuromodulators (dopamine, noradrenaline or acetylcholine  
882 to name a few) but also neuropeptides (BDNF), unconventional neurotransmitters (NO) and  
883 astrocytes surrounding neurons, which can uptake or release neurotransmitters and  
884 neuromodulators. The spectrum of the third factor of STDP is even larger since it can be  
885 extended to neurotransmitters acting as neuromodulators such as GABA and glutamate (*via*  
886 their tonic component) and endocannabinoids. Here, we reviewed the main effects of the  
887 third factor on STDP: from the emergence of STDP, to the shaping of STDP *i.e.* the  
888 dependence on  $\Delta t_{\text{STDP}}$ , and the magnitude and polarity of plasticity.

889 Beyond the time scale of  $\Delta t_{\text{STDP}}$  that is consistently in the  $\sim 80$  ms range, the studies  
890 that explored STDP properties have used a large variety of pairing protocols to induce STDP.  
891 This diversity in stimulation protocol renders the comparison between studies exceedingly  
892 difficult. As described above, beside its dependence on  $\Delta t_{\text{STDP}}$ , STDP expression is highly  
893 affected by varying the structure of STDP pairings (1:1, 1:2, ... n:n or theta bursts)  
894 (Edelmann et al., 2015), or the number and/or frequency of pairings (Sjöström et al., 2001;  
895 Cui et al., 2016) (for review see Sjöström et al., 2008; Feldman, 2012; Edelmann et al.,

896 2017). It is thus expected that the effect of neuromodulation also would strongly depend on  
897 the STDP activity pattern (as an example see Edelman et al., 2015).

898 How the local interneuron networks (GABAergic or cholinergic) or the  
899 neuromodulatory afferents are recruited and impact STDP, depends on the activity patterns of  
900 the two main inputs. *I.e.*, the third factor effect may vary with or depend on a triplet of  
901 characteristics:  $\Delta t_{\text{STDP}}$ , number of pairings, frequency of pairings. Optogenetics will most  
902 certainly be a key method to induce neuromodulator release in a more time-controlled  
903 manner to mimic for example phasic activity or explore precisely the retroactive action of  
904 neuromodulation on STDP properties.

905 The number of experimental studies investigating the signaling pathways underlying  
906 the STDP expression and their modulation by a third factor is still limited and needs further  
907 consideration. The signaling pathways underlying frequency-dependent plasticity (triggered  
908 by high- or low-frequency stimulations) have been more thoroughly explored, but need to be  
909 fully address in STDP. Signaling through G-protein coupled receptors is far more complex  
910 than the static view of the list of proteins that compose each signaling pathways. For instance,  
911 G-protein coupled receptors exhibit the "biased agonism", *i.e.* the notion that a given agonist  
912 of a signaling pathway activates only a subset of all the signaling pathways associated with  
913 its receptor (Kenakin and Christopoulos, 2013). In other words, two agonists of the same  
914 signaling pathway, even of the same receptor, activate different subsets of reactions, thus  
915 yielding different biological effects. One potential mechanism explaining biased agonism is  
916 the interplay between differential ligand-binding kinetics and the kinetics associated with  
917 different cell signaling processes (Klein Herenbrink et al., 2016). In this context, the subsets  
918 of signaling processes effectively activated by STDP pairings could differ from those  
919 activated by the stronger protocols employed in frequency-dependent plasticity.

920 The complexity of G-protein coupled receptor signaling also has consequences on  
921 STDP modulation. The available experimental data surveyed above point to a general rule  
922 according to which neuromodulation by monoamines or acetylcholine is mostly controlled by  
923 the type of G-protein coupled receptors activated: regardless of the agonist,  $G_i$ -coupled and  
924  $G_{q/11}$ -coupled receptors favor tLTD, whereas  $G_s$ - and  $G_{olf}$ -coupled receptor activation leads  
925 to tLTP. One might therefore erroneously conclude that two modulators would have the same  
926 effect by activating the same signaling pathway. This would of course be at odds with the  
927 concept that different neuromodulators exhibit different biological effects, due to different  
928 receptor affinities, different receptor locations, co-localization of diverse downstream

929 signaling molecules, and the ability of phosphorylated receptors to switch their coupling to  
930 different G proteins. Hence, dopamine signaling *via* D<sub>1</sub>R may display different biological  
931 effects from noradrenaline signaling *via*  $\beta$ -adrenergic receptors, although both activate the  
932 G<sub>s</sub>/G<sub>olf</sub> signaling pathway. Future computational models of STDP modulation should aim to  
933 reconcile the general scheme of the above rule with the specificity of neuromodulators,  
934 probably through variants of biased agonism.

935         Because of the complexity of the mode of action of neuromodulators, most of the  
936 studies have investigated the role of only a small number of neuromodulators one by one (the  
937 neuromodulator systems have mostly been activated or inhibited one-at-a-time), but the  
938 crosstalk between neuromodulators is critical, as demonstrated in only a few studies: for  
939 dopamine and acetylcholine (Brzoko et al., 2017), dopamine and GABA (Xu and Yao, 2010),  
940 dopamine and noradrenaline (Seol et al., 2007) or dopamine and endocannabinoids (Cui et  
941 al., 2015). The effects of other neurotransmitters/neuromodulators (such as adenosine,  
942 serotonin or endocannabinoids), or neuropeptides (substance P, enkephalins, oxytocin), fatty  
943 acids (arachidonic acid, cholesterol, omega-3), hormones or the role of other non-neuronal  
944 cells (astrocytes, oligodendrocytes, microglia, pericytes, ependymal cells or endothelial cells)  
945 remain to be investigated in STDP expression; Indeed, most of these actors are known to  
946 modulate rate-dependent plasticity. Furthermore, the effects of neuromodulators in STDP  
947 maintenance remain to be determined and not only for the induction phase of STDP. It has  
948 been shown in a rate-coded plasticity at CA1 hippocampal synapses that D<sub>1</sub>-like-receptor  
949 inhibition blocks late-phase LTP (Huang and Kandel, 1995), impedes consolidation of  
950 memory and accelerates its erasure (Wang et al., 2010; Lisman et al., 2011). Similarly, the  
951 third factor effect should be evaluated in the late phase of STDP (maintenance and potentially  
952 erasure).

953         By fully taking into account the third factor, *i.e.* a multicomponent learning rule, the  
954 computational power of neural networks might be considerably improved (as reviewed in  
955 Kusmierz et al., 2017). Up to now, the third factor has usually been considered in isolation  
956 from the pre- and postsynaptic firing patterns. This experimental convenience might well  
957 disguise more complex network-level properties. In this regard, the fact that the level of tonic  
958 GABA in the local network can switch STDP from Hebbian to anti-Hebbian may have  
959 important consequences in dendritic computation and in a network context (Hiratani and  
960 Fukai, 2017). The interplay between changes of the firing rate of some of the network  
961 neurons due to Hebbian STDP and resulting changes in tonic GABA could give rise to abrupt

962 STDP shifts locally from Hebbian to anti-Hebbian. Such local STDP shifts may provide the  
963 network with self-organizing properties that would not be predicted easily when the third  
964 factor is considered in isolation. Added to the fact that different synapse types in the network  
965 can have different STDP rules (and possibly, different modulation by the third factor), the  
966 complexity and variety of the resulting network dynamics would considerably increase. Note  
967 that here again, computational models will be instrumental to explore the potential impact of  
968 these mechanisms on the dynamics and functional properties of neural networks.

969 A fair criticism of the physiological relevance of STDP has been raised by Lisman et  
970 al. (2010) since *in vivo* the back-propagating action potential is obviously not triggered with a  
971 somatic current injection in the postsynaptic neuron (as classically performed in STDP  
972 experiments) but rather with the dynamic integration of synaptic inputs whose build-up  
973 would eventually reach the action potential threshold. Input-timing-dependent plasticity  
974 (ITDP), a form of heterosynaptic plasticity, consists in paired activation of presynaptic inputs  
975 separated by an interval  $\Delta t_{ITDP}$ , leading to sub- or suprathreshold activity in the postsynaptic  
976 neuron (Dudman et al., 2007; Williams et al., 2007). Therefore, ITDP could be viewed as an  
977 attractive naturalistic upgrade of STDP, not only for experimental studies (Dudman et al.,  
978 2007; Cho et al., 2012; Mehaffey and Doupe, 2015; Brandalise et al., 2016; Leroy et al.,  
979 2017) but also for computational models (Shim et al., 2016). ITDP has been reported in  
980 amygdala following activation of thalamic and cortical inputs (Humeau et al., 2003; Cho et  
981 al., 2012), in hippocampal CA1 (Dudman et al., 2007), CA2 (Leroy et al., 2017) or CA3  
982 (Brandalise et al., 2016) pyramidal cells and in avian basal ganglia (Mehaffey and Doupe,  
983 2015). Interestingly, GABA and enkephalin have been shown to modulate CA2 hippocampal  
984 ITDP (Leroy et al., 2017), which paves the way for future studies investigating the role of the  
985 third factor in ITDP properties.

986 The vast majority of STDP studies investigating the third factor have been achieved  
987 *ex vivo* (cell cultures or acute brain slices), although few studies have addressed  
988 neuromodulation of STDP *in vivo* (Mu and Poo, 2006; Cassenaer and Laurent, 2012; Schulz  
989 et al., 2010; Yagishita et al., 2014; Fisher et al., 2017). In *ex vivo* studies, neuromodulators  
990 (dopamine, acetylcholine) are typically applied exogenously because of their very low levels  
991 when compared to *in vivo*. Neuromodulators are released in tonic and phasic modes *in vivo*  
992 and therefore *ex vivo* bath-applications of neuromodulators or specific agonists hardly mimic  
993 such complexity of the neuromodulation. It would be important to explore the *in vivo*  
994 neuromodulation needed to stabilize STDP or ITDP, by transforming eligibility traces into

995 plasticity, and thus allowing an activity pattern sequence to be pertinent for the engram. Thus,  
996 there is a need to collect data *in vivo* in awake and behaving animals and model *in vivo*-like  
997 plasticity rules and stimulation patterns to fully understand the action of the third factor in  
998 Hebbian learning and information storage and recall.

## 999 **Figure Legends**

### 1000 **Figure 1: Dopamine and acetylcholine shape STDP in hippocampus and prefrontal** 1001 **cortex.**

1002 (a) Generic schematics of the main signaling pathways activated in STDP in response to  
1003 dopamine, acetylcholine and glutamate. Full and tee-shaped arrows denote activation and  
1004 inhibition, respectively. G<sub>x</sub>: G-protein coupled receptor signaling x subclass, PKA: Protein  
1005 kinase A, MEK-ERK (activation of MAPK), PP1: Protein Phosphatase-1, CaMKII: Calcium-  
1006 calmodulin dependent kinase I $\alpha$ , DAG: diacylglycerol, PLC: phospholipase C. (b) In  
1007 hippocampus, bidirectional Hebbian STDP observed in control conditions is converted to  
1008 tLTP when dopamine is applied during the STDP pairings or just after it. When dopamine is  
1009 applied 10 and 30 minutes after STDP pairings, an absence of plasticity and tLTD are  
1010 observed, respectively. Adapted from Zhang et al. (2009) and Brzosko et al. (2015).  
1011 Acetylcholine, applied during STDP pairings, converts bidirectional Hebbian STDP to  
1012 unidirectional tLTD for both post-pre and pre-post pairings. Dopamine applied just after  
1013 STDP pairings with acetylcholine during STDP pairings can rescue pre-post tLTP. Adapted  
1014 from Brzosko et al., 2017. (c) In the prefrontal cortex, addition of dopamine or D<sub>1</sub>- plus D<sub>2</sub>-  
1015 class receptor agonists to a pairing protocol that does not induce STDP promotes a  
1016 unidirectional tLTP. The inhibition of GABA<sub>A</sub> receptors or application of agonists of D<sub>2</sub>-  
1017 class receptors allows the expression of tLTP for pre-post pairings. Conversely, application of  
1018 agonists of D<sub>1</sub>-class receptors allows the expression of tLTP for post-pre pairings. Activation  
1019 of D<sub>2</sub>R expressed by GABAergic interneurons (or their direct inhibition by GABA<sub>A</sub> receptor  
1020 inhibitors) decreases activity of these interneurons uncovering tLTP for pre-post pairings. For  
1021 post-pre pairings induction relies on D<sub>1</sub>-class receptor (located on the postsynaptic neuron)  
1022 activation. Adapted from Ruan et al. (2014) and Xu and Yao (2010), with no permission  
1023 required.

1024

### 1025 **Figure 2: Noradrenaline and acetylcholine shape STDP in the visual cortex.**

1026 (a) Generic schematic of the main signaling pathways activated in STDP in response to  
1027 noradrenaline, acetylcholine and glutamate. Abbreviations are those of Figure 1a. (b) In layer

1028 2/3 of the visual cortex, STDP protocols consisting of 120 to 200 pairings at 1Hz do not  
1029 produce STDP in control conditions. When  $\alpha$ 1- and  $\beta$ -adrenergic receptor agonists (1) or  
1030 when muscarinic  $M_1R$  and  $\beta$ -adrenergic receptor agonists (3) are applied, then bidirectional  
1031 Hebbian STDP can be observed. Unidirectional anti-Hebbian tLTD and unidirectional  
1032 Hebbian tLTP are induced after  $\alpha$ 1- and  $\beta$ -adrenergic receptor agonist application,  
1033 respectively (2);  $M_1R$  agonist promotes unidirectional anti-Hebbian tLTD (3). Low and high  
1034 concentration of noradrenaline promote unidirectional anti-Hebbian tLTD (2) and  
1035 bidirectional Hebbian STDP (1), respectively. (c) Monoamines transform eligibility traces  
1036 into plasticity. Hebbian pairings (200 pairings at 10 Hz) induce post-pre tLTD and pre-post  
1037 tLTP only if serotonin and noradrenaline are released 5-10 seconds after STDP pairings.  
1038 Adapted from Seol et al. (2007), Salgado et al. (2012), Guo et al. (2012), Huang et al. (2013)  
1039 and Huang et al. (2014), He et al. (2015) with no permission required.

1040

1041 **Figure 3: GABA<sub>A</sub> and GABA<sub>B</sub> receptor activation shapes STDP in dorsal striatum and**  
1042 **hippocampus.**

1043 (a) Modulation of striatal synaptic plasticity by GABAergic signaling at different post-natal  
1044 ages. Schematic view of the impact of GABAergic signaling on corticostriatal STDP  
1045 throughout development. Left, at P<sub>7-10</sub>, inhibition of GABAergic signaling turns Hebbian  
1046 tLTD into bidirectional Hebbian STDP. Selective activation of tonic GABAergic signaling  
1047 converts Hebbian tLTD into bidirectional anti-Hebbian STDP (as observed at P<sub>25-30</sub>). Adapted  
1048 from Valtcheva et al. (2017). Right, at P<sub>25-30</sub>, inhibition of GABAergic signaling shifts  
1049 bidirectional anti-Hebbian STDP into bidirectional Hebbian STDP. Selective inhibition of  
1050 tonic GABAergic converts bidirectional anti-Hebbian STDP into Hebbian tLTD (as observed  
1051 at P<sub>7-10</sub>). Adapted from Paillé et al. (2013) and Valtcheva et al. (2017). (b) In hippocampus,  
1052 depending on the frequency of STDP pairings (5, 25 and 50Hz), inhibition of GABA<sub>A</sub> or  
1053 GABA<sub>B</sub> receptors shape differently STDP expression and polarity. GABA<sub>A</sub> receptors  
1054 modulate the timing dependence of tLTD whereas GABA<sub>B</sub> receptors control STDP frequency  
1055 dependence. Adapted from Nishiyama et al. (2010) and Sugisaki et al. (2016), with no  
1056 permission required.

1057

1058 **Figure 4: Computational models for predicting the direction of STDP have a wide range of**  
1059 **complexity. (a) Models differ in morphological complexity, from single-compartment (a1) to**  
1060 **multi-compartment models (a2). Top traces show that the back-propagating action potential**  
1061 **decreases in amplitude, initiates later and broadens as it propagates distally in multi-**

1062 compartmental models. Bottom traces show that distal synapses may produce higher calcium  
1063 elevations than proximal synapses due to higher local input resistance. **(b)** Models differ in  
1064 the mechanisms used to control calcium dynamics, from single time constant of decay, to  
1065 biophysical/biochemical models of diffusion (red arrows), pumps (such as the plasma  
1066 membrane ATPase: PMCA) that extrude calcium (yellow arrow), buffers (such as  
1067 calmodulin, calbindin, or immobile buffers) that bind to free calcium (gray arrows), and  
1068 calcium release (not shown). All models include influx through the NMDA receptors (blue  
1069 arrows). **(c)** The prediction of plasticity from calcium often uses two amplitude thresholds  
1070 **(c1)**, but sometimes include duration thresholds **(c2)** or other measures of calcium duration.  
1071  $T_{LTP}$ : tLTP amplitude threshold,  $T_{LTD}$ : tLTD amplitude threshold,  $D_{LTD}$ : threshold on the  
1072 duration of the calcium elevation.

1073

1074 **Figure 5: Main predictions of the model of Cui et al. (2016).** **(a)** Scheme of the signaling  
1075 pathways that are considered in the model. The postsynaptic weight is set by the amount of  
1076 phosphorylated CaMKII whereas the presynaptic weight is controlled by the activation of  
1077  $CB_1R$ . Abbreviations: PIP2: phosphatidylinositol 4,5-bisphosphate; DAG: diacylglycerol; IP3:  
1078 inositol-1,4,5-trisphosphate;  $PLC\beta/\delta$ : phospholipase-C $\beta/\delta$ ;  $DAGL\alpha$ : diacylglycerol lipase  $\alpha$ ;  
1079 2-AG: 2-arachidonoylglycerol; AEA: anandamide; TRPV1: transient receptor potential cation  
1080 channel subfamily V member 1; IP3R: IP3-receptor channel; SERCA:  
1081 sarcoplasmic/endoplasmic reticulum calcium ATPase;  $Ca_{ER}$ : calcium in the endoplasmic  
1082 reticulum;  $(Ca)_4CaM$ : fully bound calmodulin; CaN: calcineurin aka PP2B; PKA: protein  
1083 kinase A; I1p/I1: phosphorylated/unphosphorylated protein phosphatase-1 inhibitor 1  
1084 (DARPP-32 in striatal output neurons); PP1: protein phosphatase 1; CaMKII:  
1085  $Ca^{2+}$ /calmodulin-dependent protein kinase II. **(b)** Prediction of the evolution of the total  
1086 synaptic weight (product of the pre- and postsynaptic weights) when the spike timing and the  
1087 number of pairing varies. tLTP progressively emerges at positive  $\Delta t_{STDP}$ , whereas for  
1088 negative  $\Delta t_{STDP}$ , the model correctly predicts two domains of tLTP, one around 10-20  
1089 pairings and another emerging after 50 pairings. **(c)** When  $CB_1R$  are blocked in the model,  
1090 both the tLTD and the tLTP for low pairing numbers disappear. **(d)** Adding presynaptic  $D_2Rs$   
1091 in the model, correctly predicts that tLTP for low pairing numbers is also controlled by  
1092 dopamine. Adapted from Cui et al. (2016) with no permission required.

1093

1094

1095 **Author contributions**

1096 AF and AM participated in the writing of the neuromodulators section; JJ, HB and KB wrote  
1097 the "Molecular pathway-based computational models of STDP " section; SV wrote the  
1098 "Modulation of STDP by astrocytes: the forgotten third factor " section; LV wrote the  
1099 introduction, neuromodulators and conclusion sections; all authors have edited and corrected  
1100 the manuscript.

1101

1102 **Abbreviations**

1103 STDP: spike-timing dependent plasticity; NMDAR: N-methyl-D-aspartate receptor; BDNF:  
1104 brain-derived neurotrophic factor; GABA: gamma-aminobutyric acid; tLTD: timing-  
1105 dependent long term depression; tLTP: timing-dependent long term potentiation; CB<sub>1</sub>R:  
1106 cannabinoid type-1 receptor; D<sub>x</sub>R: dopaminergic type-X receptor; M<sub>x</sub>: muscarinic type-X  
1107 receptor; cAMP: cyclic adenosine monophosphate; nAChRs: Nicotinic acetylcholine  
1108 receptors; mAChRs: Muscarinic acetylcholine receptors; NO: nitric oxide; cGMP: cyclic  
1109 guanosine monophosphate; DARP-32: dopamine- and cAMP-regulated phosphoprotein, Mr  
1110 32 kDa; AMPAR:  $\alpha$ -amino-3-hydroxy-5-methyl-4-isoxazolepropionic acid receptor ;  
1111 EAAT2: excitatory amino acid transporter-2; mGluR: metabotropic glutamatergic receptor;  
1112 ATP: adenosine triphosphate; CaMKII: Ca<sup>2+</sup>/calmodulin-dependent protein kinase-II; ERK:  
1113 extracellular signal-regulated kinase; ITDP: input-timing dependent plasticity.

1114

1115 **Acknowledgments:** This work was supported by grants from the Agence Nationale pour la  
1116 Recherche (ANR-CRCNS Dopaciumcity) and the LabEx Paris-Sciences et Lettres (PSL).  
1117 AM was supported by the Fondation pour la Recherche Médicale (FRM). KTB and JZ were  
1118 supported by the joint NIH-NSF CRCNS program through NIAAA grant R01DA03889.

1119

1120 **Competing financial interests:** The authors declare no competing financial interests.

1121

1122 **References**

- 1123  
1124 Abbott, L.F., Nelson, S.B., 2000. Synaptic plasticity: taming the beast. *Nat. Neurosci.* 3, 1178.  
1125 <https://doi.org/10.1038/81453>
- 1126 Ade K.K., Janssen M.J., Ortinski P.I., Vicini S., 2008. Differential tonic GABA conductances in  
1127 striatal medium spiny neurons. *J Neurosci.* 2008. 28, 1185-1197.  
1128 <https://doi.org/10.1523/JNEUROSCI.3908-07.2008>
- 1129 Ahumada, J., de Sevilla, D.F., Couve, A., Buño, W., Fuenzalida, M., 2013. Long-term depression of  
1130 inhibitory synaptic transmission induced by spike-timing dependent plasticity requires  
1131 coactivation of endocannabinoid and muscarinic receptors. *Hippocampus* 23, 1439–1452.  
1132 <https://doi.org/10.1002/hipo.22196>
- 1133 Albuquerque, E.X., Pereira, E.F.R., Alkondon, M., Rogers, S.W., 2009. Mammalian Nicotinic  
1134 Acetylcholine Receptors: From Structure to Function. *Physiol. Rev.* 89, 73–120.  
1135 <https://doi.org/10.1152/physrev.00015.2008>
- 1136 Andrade-Talavera, Y., Duque-Feria, P., Paulsen, O., Rodríguez-Moreno, A., 2016. Presynaptic  
1137 Spike Timing-Dependent Long-Term Depression in the Mouse Hippocampus. *Cereb. Cortex N.Y.*  
1138 26, 3637. <https://doi.org/10.1093/cercor/bhw172>
- 1139 Araque, A., Carmignoto, G., Haydon, P.G., Oliet, S.H.R., Robitaille, R., Volterra, A., 2014.  
1140 Gliotransmitters travel in time and space. *Neuron* 81, 728–739.  
1141 <https://doi.org/10.1016/j.neuron.2014.02.007>
- 1142 Bannon, N.M., Chistiakova, M., Chen, J.-Y., Bazhenov, M., Volgushev, M., 2017. Adenosine Shifts  
1143 Plasticity Regimes between Associative and Homeostatic by Modulating Heterosynaptic  
1144 Changes. *J. Neurosci. Off. J. Soc. Neurosci.* 37, 1439–1452.  
1145 <https://doi.org/10.1523/JNEUROSCI.2984-16.2016>
- 1146 Bar-Ilan, L., Gidon, A., Segev, I., 2013. The role of dendritic inhibition in shaping the plasticity of  
1147 excitatory synapses. *Front. Neural Circuits* 6, 118. <https://doi.org/10.3389/fncir.2012.00118>
- 1148 Bell, C.C., Han, V.Z., Sugawara, Y., Grant, K., 1997. Synaptic plasticity in a cerebellum-like  
1149 structure depends on temporal order. *Nature* 387, 278–281.  
1150 <https://doi.org/10.1038/387278a0>
- 1151 Bender, V.A., Bender, K.J., Brasier, D.J., Feldman, D.E., 2006. Two Coincidence Detectors for Spike  
1152 Timing-Dependent Plasticity in Somatosensory Cortex. *J. Neurosci. Off. J. Soc. Neurosci.* 26, 4166.  
1153 <https://doi.org/10.1523/JNEUROSCI.0176-06.2006>
- 1154 Bernardinelli Y., Muller D., Nikonenko I., 2014. Astrocyte-synapse structural plasticity. *Neural*  
1155 *Plast.* 2014, 232105. <https://doi.org/10.1155/2014/232105>
- 1156 Bi, G., Poo, M., 1998. Synaptic Modifications in Cultured Hippocampal Neurons: Dependence on  
1157 Spike Timing, Synaptic Strength, and Postsynaptic Cell Type. *J. Neurosci.* 18, 10464–10472.

- 1158 Bissière, S., Humeau, Y., Lüthi, A., 2003. Dopamine gates LTP induction in lateral amygdala by  
1159 suppressing feedforward inhibition. *Nat. Neurosci.* 6, 587–592.  
1160 <https://doi.org/10.1038/nn1058>
- 1161 Brandalise, F., Carta, S., Helmchen, F., Lisman, J., Gerber, U., 2016. Dendritic NMDA spikes are  
1162 necessary for timing-dependent associative LTP in CA3 pyramidal cells. *Nat. Commun.* 7, 13480.  
1163 <https://doi.org/10.1038/ncomms13480>  
1164
- 1165 Brzosko, Z., Schultz, W., Paulsen, O., 2015. Retroactive modulation of spike timing-dependent  
1166 plasticity by dopamine. *eLife* 4. <https://doi.org/10.7554/eLife.09685>  
1167
- 1168 Brzosko, Z., Zannone, S., Schultz, W., Clopath, C., Paulsen, O., 2017. Sequential neuromodulation  
1169 of Hebbian plasticity offers mechanism for effective reward-based navigation, *eLife* 6.  
1170 <https://doi.org/10.7554/eLife.27756>  
1171
- 1172 Bush, D., Jin, Y., 2012. Calcium control of triphasic hippocampal STDP. *J. Comput. Neurosci.* 33,  
1173 495–514. <https://doi.org/10.1007/s10827-012-0397-5>
- 1174 Calabresi, P., Picconi, B., Tozzi, A., Ghiglieri, V., Di Filippo, M., 2014. Direct and indirect pathways  
1175 of basal ganglia: a critical reappraisal. *Nat. Neurosci.* 17, 1022–1030.  
1176 <https://doi.org/10.1038/nn.3743>
- 1177 Carlson, K.D., Giordano, N., 2011. Interplay of the magnitude and time-course of postsynaptic  
1178 Ca<sup>2+</sup> concentration in producing spike timing-dependent plasticity. *J. Comput. Neurosci.* 30,  
1179 747–758. <https://doi.org/10.1007/s10827-010-0290-z>
- 1180 Cassenaer, S., Laurent, G., 2012. Conditional modulation of spike-timing-dependent plasticity for  
1181 olfactory learning. *Nature* 482, 47–52. <https://doi.org/10.1038/nature10776>
- 1182 Cho, J.H., Bayazitov, I.T., Meloni, E.G., Myers, K.M., Carlezon, W.A. Jr., Zakharenko, S.S., Bolshakov,  
1183 V.Y., 2011. Coactivation of thalamic and cortical pathways induces input timing-dependent  
1184 plasticity in amygdala. *Nat. Neurosci.* 15, 113. <https://doi.org/10.1038/nn.2993>  
1185
- 1186 Chung, W.-S., Welsh, C.A., Barres, B.A., Stevens, B., 2015. Do glia drive synaptic and cognitive  
1187 impairment in disease? *Nat. Neurosci.* 18, 1539–1545. <https://doi.org/10.1038/nn.4142>
- 1188 Clopath, C., Büsing, L., Vasilaki, E., Gerstner, W., 2010. Connectivity reflects coding: a model of  
1189 voltage-based STDP with homeostasis. *Nat. Neurosci.* 13, 344–352.  
1190 <https://doi.org/10.1038/nn.2479>
- 1191 Corlew, R., Wang, Y., Ghermazien, H., Erisir, A., Philpot, B.D., 2007. Developmental Switch in the  
1192 Contribution of Presynaptic and Postsynaptic NMDA Receptors to Long-Term Depression. *J.*  
1193 *Neurosci.* 27, 9835–9845. <https://doi.org/10.1523/JNEUROSCI.5494-06.2007>
- 1194 Couey, J.J., Meredith, R.M., Spijker, S., Poorthuis, R.B., Smit, A.B., Brussaard, A.B., Mansvelder,  
1195 H.D., 2007. Distributed Network Actions by Nicotine Increase the Threshold for Spike-Timing-  
1196 Dependent Plasticity in Prefrontal Cortex. *Neuron* 54, 73–87.  
1197 <https://doi.org/10.1016/j.neuron.2007.03.006>

- 1198 Cui, Y., Paillé, V., Xu, H., Genet, S., Delord, B., Fino, E., Berry, H., Venance, L., 2015.  
1199 Endocannabinoids mediate bidirectional striatal spike-timing-dependent plasticity. *J. Physiol.*  
1200 593, 2833–2849. <https://doi.org/10.1113/JP270324>
- 1201 Cui, Y., Prokin, I., Xu, H., Delord, B., Genet, S., Venance, L., Berry, H., 2016. Endocannabinoid  
1202 dynamics gate spike-timing dependent depression and potentiation. *eLife* 5.  
1203 <https://doi.org/10.7554/eLife.13185>
- 1204 Cui, Y., Prokin, I., Mendes, A., Berry, H., Venance, L., 2018. Robustness of STDP to spike timing  
1205 jitter. *Scientific Reports* 8: 8139.  
1206 Doi: 10.1038/s41598-018-26436-y  
1207
- 1208 Cutsuridis, V., 2011. GABA inhibition modulates NMDA-R mediated spike timing dependent  
1209 plasticity (STDP) in a biophysical model. *Neural Netw. Off. J. Int. Neural Netw. Soc.* 24, 29–42.  
1210 <https://doi.org/10.1016/j.neunet.2010.08.005>
- 1211 Cutsuridis V., 2012. Bursts shape the NMDA-R mediated spike timing dependent plasticity  
1212 curve: role of burst interspike interval and GABAergic inhibition. *Cogn Neurodyn.* 6, 421–41.  
1213 <https://doi.org/10.1007/s11571-012-9205-1>
- 1214 Dan, Y., Poo, M.-M., 2006. Spike timing-dependent plasticity: from synapse to perception.  
1215 *Physiol. Rev.* 86, 1033–1048. <https://doi.org/10.1152/physrev.00030.2005>
- 1216 Danbolt, N.C., 2001. Glutamate uptake. *Prog. Neurobiol.* 65, 1–105.
- 1217 Day, M., Wokosin, D., Plotkin, J.L., Tian, X., Surmeier, D.J., 2008. Differential Excitability and  
1218 Modulation of Striatal Medium Spiny Neuron Dendrites. *J. Neurosci.* 28, 11603–11614.  
1219 <https://doi.org/10.1523/JNEUROSCI.1840-08.2008>
- 1220 De Pittà, M., Volman, V., Berry, H., Ben-Jacob, E., 2011. A tale of two stories: astrocyte regulation  
1221 of synaptic depression and facilitation. *PLoS Comput. Biol.* 7, e1002293.  
1222 <https://doi.org/10.1371/journal.pcbi.1002293>  
1223
- 1224 De Pittà, M., Volman, V., Berry, H., Parpura V, Volterra, A., Ben-Jacob, E., 2012. Computational  
1225 quest for understanding the role of astrocyte signaling in synaptic transmission and plasticity.  
1226 *Front. Comput. Neurosci.* 6, 98. <https://doi.org/10.3389/fncom.2012.00098>  
1227
- 1228 De Pittà, M., Brunel, N., 2016. Modulation of Synaptic Plasticity by Glutamatergic  
1229 Gliotransmission: A Modeling Study. *Neural Plast.* 2016, 7607924.  
1230 <https://doi.org/10.1155/2016/7607924>
- 1231 Debanne, D., Gähwiler, B.H., Thompson, S.M., 1998. Long-term synaptic plasticity between pairs  
1232 of individual CA3 pyramidal cells in rat hippocampal slice cultures. *J. Physiol.* 507, 237.  
1233 <https://doi.org/10.1111/j.1469-7793.1998.237bu.x>
- 1234 Debanne, D., Gähwiler, B.H., Thompson, S.M., 1997. Bidirectional Associative Plasticity of Unitary  
1235 CA3-CA1 EPSPs in the Rat Hippocampus In Vitro. *J. Neurophysiol.* 77, 2851–2855.  
1236 <https://doi.org/10.1152/jn.1997.77.5.2851>

- 1237 Dudman, J.T., Tsay, D., Siegelbaum, S.A., 2007. A role for synaptic inputs at distal dendrites:  
1238 instructive signals for hippocampal long-term plasticity. *Neuron*. 56, 866.  
1239 <https://doi.org/10.1016/j.neuron.2007.10.020>  
1240
- 1241 Edelmann, E., Lessmann, V., 2011. Dopamine Modulates Spike Timing-Dependent Plasticity and  
1242 Action Potential Properties in CA1 Pyramidal Neurons of Acute Rat Hippocampal Slices. *Front.*  
1243 *Synaptic Neurosci.* 3. <https://doi.org/10.3389/fnsyn.2011.00006>
- 1244 Edelmann, E., Lessmann, V., 2013. Dopamine regulates intrinsic excitability thereby gating  
1245 successful induction of spike timing-dependent plasticity in CA1 of the hippocampus. *Front.*  
1246 *Neurosci.* 7. <https://doi.org/10.3389/fnins.2013.00025>
- 1247 Edelmann, E., Leßmann, V., Brigadski, T., 2014. Pre- and postsynaptic twists in BDNF secretion  
1248 and action in synaptic plasticity. *Neuropharmacology, BDNF Regulation of Synaptic Structure,*  
1249 *Function, and Plasticity* 76, 610–627. <https://doi.org/10.1016/j.neuropharm.2013.05.043>
- 1250 Edelmann, E., Cepeda-Prado, E., Franck, M., Lichtenecker, P., Brigadski, T., and Lessmann, V.,  
1251 2015. Theta burst firing recruits BDNF release and signaling in postsynaptic CA1 neurons in  
1252 spike-timing-dependent LTP. *Neuron* 86, 1041–1054.  
1253 <https://doi.org/10.1016/j.neuron.2015.04.007>
- 1254 Edelmann E, Cepeda-Prado E, Leßmann V., 2017. Coexistence of Multiple Types of Synaptic  
1255 Plasticity in Individual Hippocampal CA1 Pyramidal Neurons. *Front Synaptic Neurosci.* 9,  
1256 7. <https://doi.org/10.3389/fnsyn.2017.00007>
- 1257 Egger, V., Feldmeyer, D., Sakmann, B., 1999. Coincidence detection and changes of synaptic  
1258 efficacy in spiny stellate neurons in rat barrel cortex. *Nat. Neurosci.* 2, 1098–1105.  
1259 <https://doi.org/10.1038/16026>
- 1260 Evans, R.C., Blackwell, K.T., 2015. Calcium: amplitude, duration, or location? *Biol. Bull.* 228, 75–  
1261 83. <https://doi.org/10.1086/BBLv228n1p75>
- 1262 Evans, R.C., Morera-Herreras, T., Cui, Y., Du, K., Sheehan, T., Kotaleski, J.H., Venance, L., Blackwell,  
1263 K.T., 2012. The Effects of NMDA Subunit Composition on Calcium Influx and Spike Timing-  
1264 Dependent Plasticity in Striatal Medium Spiny Neurons. *PLoS Comput. Biol.* 8.  
1265 <https://doi.org/10.1371/journal.pcbi.1002493>
- 1266 Feldman, D.E., 2012. The Spike-Timing Dependence of Plasticity. *Neuron* 75, 556–571.  
1267 <https://doi.org/10.1016/j.neuron.2012.08.001>
- 1268 Feldman, D.E., 2000. Timing-based LTP and LTD at vertical inputs to layer II/III pyramidal cells  
1269 in rat barrel cortex. *Neuron* 27, 45–56.
- 1270 Fino, E., Deniau, J.-M., Venance, L., 2008. Cell-specific spike-timing-dependent plasticity in  
1271 GABAergic and cholinergic interneurons in corticostriatal rat brain slices. *J. Physiol.* 586, 265.  
1272 <https://doi.org/10.1113/jphysiol.2007.144501>
- 1273 Fino, E., Glowinski, J., Venance, L., 2005. Bidirectional activity-dependent plasticity at  
1274 corticostriatal synapses. *J. Neurosci. Off. J. Soc. Neurosci.* 25, 11279–11287.  
1275 <https://doi.org/10.1523/JNEUROSCI.4476-05.2005>

- 1276 Fino, E., Paille, V., Cui, Y., Morera-Herreras, T., Deniau, J.-M., Venance, L., 2010. Distinct  
1277 coincidence detectors govern the corticostriatal spike timing-dependent plasticity. *J. Physiol.*  
1278 588, 3045–3062. <https://doi.org/10.1113/jphysiol.2010.188466>
- 1279 Fino, E., Paille, V., Deniau, J.-M., Venance, L., 2009. Asymmetric spike-timing dependent plasticity  
1280 of striatal nitric oxide-synthase interneurons. *Neuroscience* 160, 744–754.  
1281 <https://doi.org/10.1016/j.neuroscience.2009.03.015>
- 1282 Fisher, S.D., Robertson, P.B., Black, M.J., Redgrave, P., Sagar, M.A., Abraham, W.C., Reynolds, J.N.J.,  
1283 2017. Reinforcement determines the timing dependence of corticostriatal synaptic plasticity in  
1284 vivo. *Nat. Commun.* 8. <https://doi.org/10.1038/s41467-017-00394-x>
- 1285 Fossat, P., Turpin, F.R., Sacchi, S., Dulong, J., Shi, T., Rivet, J.-M., Sweedler, J.V., Pollegioni, L.,  
1286 Millan, M.J., Oliet, S.H.R., Mothet, J.-P., 2011. Glial D-serine gates NMDA receptors at excitatory  
1287 synapses in prefrontal cortex. *Cereb. Cortex N. Y. N 1991* 22, 595–606.  
1288 <https://doi.org/10.1093/cercor/bhr130>
- 1289 Frémaux, N., Gerstner, W., 2015. Neuromodulated Spike-Timing-Dependent Plasticity, and  
1290 Theory of Three-Factor Learning Rules. *Front. Neural Circuits* 9.  
1291 <https://doi.org/10.3389/fncir.2015.00085>
- 1292 Froemke, R.C., Poo, M., Dan, Y., 2005. Spike-timing-dependent synaptic plasticity depends on  
1293 dendritic location. *Nature* 434, 221–225. <https://doi.org/10.1038/nature03366>
- 1294 Froemke R.C., 2015. Plasticity of cortical excitatory-inhibitory balance. *Annu Rev Neurosci.*  
1295 38:195–219.
- 1296 Gerstner, W., Lehmann, M., Liakoni, V., Corneil, D., Brea, J., 2018. Eligibility Traces and Plasticity  
1297 on Behavioral Time Scales: Experimental Support of neoHebbian Three-Factor Learning Rules.  
1298 arXiv:1801.05219v1 [q-bio.NC]  
1299
- 1300 Gilson, M., Fukai, T., 2011. Stability versus Neuronal Specialization for STDP: Long-Tail Weight  
1301 Distributions Solve the Dilemma. *PloS One.* 6, e25339.  
1302 <https://doi.org/10.1371/journal.pone.0025339>  
1303
- 1304 Gjorgjieva, J., Clopath, C., Audet, J., Pfister, J.-P., 2011. A triplet spike-timing-dependent plasticity  
1305 model generalizes the Bienenstock-Cooper-Munro rule to higher-order spatiotemporal  
1306 correlations. *Proc. Natl. Acad. Sci. U. S. A.* 108, 19383–19388.  
1307 <https://doi.org/10.1073/pnas.1105933108>
- 1308 Goriounova, N.A., Mansvelder, H.D., 2012. Nicotine Exposure during Adolescence Leads to Short-  
1309 and Long-Term Changes in Spike Timing-Dependent Plasticity in Rat Prefrontal Cortex. *J.*  
1310 *Neurosci.* 32, 10484–10493. <https://doi.org/10.1523/JNEUROSCI.5502-11.2012>
- 1311 Graupner, M., Brunel, N., 2012. Calcium-based plasticity model explains sensitivity of synaptic  
1312 changes to spike pattern, rate, and dendritic location. *Proc. Natl. Acad. Sci. U. S. A.* 109, 3991–  
1313 3996. <https://doi.org/10.1073/pnas.1109359109>

- 1314 Graupner, M., Brunel, N., 2010. Mechanisms of induction and maintenance of spike-timing  
1315 dependent plasticity in biophysical synapse models. *Front. Comput. Neurosci.* 4.  
1316 <https://doi.org/10.3389/fncom.2010.00136>
- 1317 Graupner, M., Brunel, N., 2007. STDP in a bistable synapse model based on CaMKII and  
1318 associated signaling pathways. *PLoS Comput. Biol.* 3, e221.  
1319 <https://doi.org/10.1371/journal.pcbi.0030221>
- 1320 Graupner, M., Wallisch, P., Ostojic, S., 2016. Natural Firing Patterns Imply Low Sensitivity of  
1321 Synaptic Plasticity to Spike Timing Compared with Firing Rate. *J. Neurosci. Off. J. Soc. Neurosci.*  
1322 36, 11238–11258. <https://doi.org/10.1523/JNEUROSCI.0104-16.2016>
- 1323 Griffith T., Mellor J., Tsaneva-Atanasova K., 2015. Spike-Timing Dependent Plasticity (STDP),  
1324 Biophysical Models. In: Jaeger D., Jung R. (eds) *Encyclopedia of Computational Neuroscience*.  
1325 Springer, New York, NY
- 1326 Griffith, T., Tsaneva-Atanasova, K., Mellor, J.R., 2016. Control of Ca<sup>2+</sup> Influx and Calmodulin  
1327 Activation by SK-Channels in Dendritic Spines. *PLoS Comput. Biol.* 12, e1004949.  
1328 <https://doi.org/10.1371/journal.pcbi.1004949>
- 1329 Groen, M.R., Paulsen, O., Pérez-Garci, E., Nevian, T., Wortel, J., Dekker, M.P., Mansvelder, H.D., van  
1330 Ooyen, A., Meredith, R.M., 2014. Development of dendritic tonic GABAergic inhibition regulates  
1331 excitability and plasticity in CA1 pyramidal neurons. *J. Neurophysiol.* 112, 287–299.  
1332 <https://doi.org/10.1152/jn.00066.2014>
- 1333 Guo, Y., Huang, S., Pasquale, R. de, McGehrin, K., Lee, H.-K., Zhao, K., Kirkwood, A., 2012. dark  
1334 exposure extends the integration window for spike-timing dependent plasticity. *J. Neurosci. Off.*  
1335 *J. Soc. Neurosci.* 32, 15027. <https://doi.org/10.1523/JNEUROSCI.2545-12.2012>
- 1336 Haj-Dahmane, S., Béïque, J.C., Shen, R.-Y., 2017. GluA2-Lacking AMPA Receptors and Nitric Oxide  
1337 Signaling Gate Spike-Timing–Dependent Potentiation of Glutamate Synapses in the Dorsal  
1338 Raphe Nucleus. *eNeuro* 4. <https://doi.org/10.1523/ENEURO.0116-17.2017>
- 1339 Han, V.Z., Grant, K., Bell, C.C., 2000. Reversible Associative Depression and Nonassociative  
1340 Potentiation at a Parallel Fiber Synapse. *Neuron* 27, 611–622. [https://doi.org/10.1016/S0896-6273\(00\)00070-2](https://doi.org/10.1016/S0896-6273(00)00070-2)
- 1342 Hardingham, N., Dachtler, J., Fox, K., 2013. The role of nitric oxide in pre-synaptic plasticity and  
1343 homeostasis. *Front. Cell. Neurosci.* 7. <https://doi.org/10.3389/fncel.2013.00190>
- 1344 Hardingham, N., Fox, K., 2006. The Role of Nitric Oxide and GluR1 in Presynaptic and  
1345 Postsynaptic Components of Neocortical Potentiation. *J. Neurosci.* 26, 7395–7404.  
1346 <https://doi.org/10.1523/JNEUROSCI.0652-06.2006>
- 1347 He, K., Huertas, M., Hong, S.Z., Tie, X., Hell, J.W., Shouval, H., Kirkwood, A., 2015. Distinct  
1348 Eligibility Traces for LTP and LTD in Cortical Synapses. *Neuron* 88, 528-538.  
1349 <https://doi.org/10.1016/j.neuron.2015.09.037>
- 1350

- 1351 Henneberger, C., Papouin, T., Oliet, S.H.R., Rusakov, D.A., 2010. Long-term potentiation depends  
1352 on release of D-serine from astrocytes. *Nature* 463, 232–236.  
1353 <https://doi.org/10.1038/nature08673>
- 1354 Higley, M.J., Sabatini, B.L., 2010. Competitive regulation of synaptic Ca<sup>2+</sup> influx by D2 dopamine  
1355 and A2A adenosine receptors. *Nat. Neurosci.* 13, 958–966. <https://doi.org/10.1038/nn.2592>
- 1356 Hiratani N, Fukai T., 2017. Detailed Dendritic Excitatory/Inhibitory Balance through  
1357 Heterosynaptic Spike-Timing-Dependent Plasticity. *J. Neurosci.* 37, 12106-  
1358 12122. <https://doi.org/10.1523/JNEUROSCI.0027-17.2017>
- 1359 Huang, Y.Y., Kandel, E.R., 1995. D1/D5 receptor agonists induce a protein synthesis-dependent  
1360 late potentiation in the CA1 region of the hippocampus. *Proc. Natl. Acad. Sci. U. S. A.* 92, 2446-  
1361 2450.
- 1362  
1363 Huang, S., Hugarir, R.L., Kirkwood, A., 2013. Adrenergic Gating of Hebbian Spike-Timing-  
1364 Dependent Plasticity in Cortical Interneurons. *J. Neurosci.* 33, 13171–13178.  
1365 <https://doi.org/10.1523/JNEUROSCI.5741-12.2013>
- 1366 Huang, S., Rozas, C., Treviño, M., Contreras, J., Yang, S., Song, L., Yoshioka, T., Lee, H.-K.,  
1367 Kirkwood, A., 2014. Associative Hebbian synaptic plasticity in primate visual cortex. *J. Neurosci.*  
1368 *Off. J. Soc. Neurosci.* 34, 7575–7579. <https://doi.org/10.1523/JNEUROSCI.0983-14.2014>
- 1369 Humeau, Y., Shaban, H., Bissière, S., Lüthi, A., 2003. Presynaptic induction of heterosynaptic  
1370 associative plasticity in the mammalian brain. *Nature.* 426, 841-845.  
1371 <https://doi.org/10.1038/nature02194>
- 1372  
1373 Inglis, F.M., Moghaddam, B., 1999. Dopaminergic innervation of the amygdala is highly  
1374 responsive to stress. *J. Neurochem.* 72, 1088–1094.
- 1375 Izhikevich, E.M., 2007. Solving the Distal Reward Problem through Linkage of STDP and  
1376 Dopamine Signaling. *Cereb. Cortex* 17, 2443–2452. <https://doi.org/10.1093/cercor/bhl152>
- 1377 Jędrzejewska-Szmek, J., Damodaran, S., Dorman, D.B., Blackwell, K.T., 2016. Calcium dynamics  
1378 predict direction of synaptic plasticity in striatal spiny projection neurons. *Eur. J. Neurosci.* 45,  
1379 1044–1056. <https://doi.org/10.1111/ejn.13287>
- 1380 Jones, C.K., Byun, N., Bubser, M., 2012. Muscarinic and nicotinic acetylcholine receptor agonists  
1381 and allosteric modulators for the treatment of schizophrenia. *Neuropsychopharmacol. Off. Publ.*  
1382 *Am. Coll. Neuropsychopharmacol.* 37, 16–42. <https://doi.org/10.1038/npp.2011.199>
- 1383 Kempter, R., Gerstner, W., van Hemmen, J.L., 1998. How the threshold of a neuron determines its  
1384 capacity for coincidence detection. *Biosystems* 48, 105–112. [https://doi.org/10.1016/S0303-  
1385 2647\(98\)00055-0](https://doi.org/10.1016/S0303-2647(98)00055-0)
- 1386 Kenakin, T., Christopoulos, A., 2013. Signalling bias in new drug discovery: detection,  
1387 quantification and therapeutic impact. *Nat. Rev. Drug. Discov.* 12, 205-216.  
1388 <https://doi.org/10.1038/nrd3954>

- 1389 Klein Herenbrink, C., Sykes D.A., Donthamsetti, P., Canals, M., Coudrat, T., Shonberg, J.,  
1390 Scammells, P.J., Capuano, B., Sexton, P.M., Charlton, S.J., Javitch, J.A., Christopoulos, A., Lane J.R.,  
1391 2016. The role of kinetic context in apparent biased agonism at GPCRs. *Nat. Commun.* 7, 10842.  
1392 <https://doi.org/10.1038/ncomms10842>
- 1393 Koester, H.J., Sakmann, B., 1998. Calcium dynamics in single spines during coincident pre- and  
1394 postsynaptic activity depend on relative timing of back-propagating action potentials and  
1395 subthreshold excitatory postsynaptic potentials. *Proc. Natl. Acad. Sci. U. S. A.* 95, 9596.
- 1396 Korte, M., Schmitz, D., 2016. Cellular and System Biology of Memory: Timing, Molecules, and  
1397 Beyond. *Physiol. Rev.* 96, 647–693. <https://doi.org/10.1152/physrev.00010.2015>
- 1398 Kumar, A., Mehta, M.R., 2011. Frequency-Dependent Changes in NMDAR-Dependent Synaptic  
1399 Plasticity. *Front. Comput. Neurosci.* 5, 38. <https://doi.org/10.3389/fncom.2011.00038>
- 1400 Kuśmierz, Ł., Isomura, T., Toyoizumi, T., 2017. Learning with three factors: modulating Hebbian  
1401 plasticity with errors. *Curr. Opin. Neurobiol., Computational Neuroscience* 46, 170–177.  
1402 <https://doi.org/10.1016/j.conb.2017.08.020>
- 1403 Lerner, T.N., Horne, E.A., Stella, N., Kreitzer, A.C., 2010. Endocannabinoid signaling mediates  
1404 psychomotor activation by adenosine A2A antagonists. *J. Neurosci. Off. J. Soc. Neurosci.* 30,  
1405 2160–2164. <https://doi.org/10.1523/JNEUROSCI.5844-09.2010>
- 1406 Leroy, F., Brann, D.H., Meira, T., Siegelbaum, S.A., 2017. Input-Timing-Dependent Plasticity in the  
1407 Hippocampal CA2 Region and Its Potential Role in Social Memory. *Neuron.* 95, 1089-1102.e5.  
1408 <https://doi.org/10.1016/j.neuron.2017.07.036>
- 1409
- 1410 Letzkus, J.J., Kampa, B.M., Stuart, G.J., 2006. Learning Rules for Spike Timing-Dependent  
1411 Plasticity Depend on Dendritic Synapse Location. *J. Neurosci.* 26, 10420–10429.  
1412 <https://doi.org/10.1523/JNEUROSCI.2650-06.2006>
- 1413 Lin, Y.-W., Min, M.-Y., Chiu, T.-H., Yang, H.-W., 2003. Enhancement of Associative Long-Term  
1414 Potentiation by Activation of  $\beta$ -Adrenergic Receptors at CA1 Synapses in Rat Hippocampal  
1415 Slices. *J. Neurosci.* 23, 4173–4181.
- 1416 Lisman, J., Grace, A.A., Duzel, E., 2011. A neoHebbian framework for episodic memory; role of  
1417 dopamine-dependent late LTP. *Trends Neurosci.* 34, 536-547.  
1418 <https://doi.org/10.1016/j.tins.2011.07.006>
- 1419
- 1420 Lu, H., Park, H., Poo, M.-M., 2014. Spike-timing-dependent BDNF secretion and synaptic  
1421 plasticity. *Phil Trans R Soc B* 369, 20130132. <https://doi.org/10.1098/rstb.2013.0132>
- 1422 Lu, J., Li, C., Zhao, J.-P., Poo, M., Zhang, X., 2007. Spike-Timing-Dependent Plasticity of Neocortical  
1423 Excitatory Synapses on Inhibitory Interneurons Depends on Target Cell Type. *J. Neurosci.* 27,  
1424 9711–9720. <https://doi.org/10.1523/JNEUROSCI.2513-07.2007>
- 1425 Ma, S., Hangya, B., Leonard, C.S., Wisden, W., Gundlach, A.L., 2018. Dual-transmitter systems  
1426 regulating arousal, attention, learning and memory. *Neurosci. Biobehav. Rev.*, SI: 2016 IBNS  
1427 Meeting 85, 21–33. <https://doi.org/10.1016/j.neubiorev.2017.07.009>

- 1428 Magee, J.C., Johnston, D., 1997. A synaptically controlled, associative signal for Hebbian plasticity  
1429 in hippocampal neurons. *Science* 275, 209–213.
- 1430 Mathur, B. N. & Lovinger, D. M., 2012. Endocannabinoid–Dopamine Interactions in Striatal  
1431 Synaptic Plasticity. *Front. Pharmacol.* 3. <https://doi.org/10.3389/fphar.2012.00066>
- 1432 Markram, H., Lübke, J., Frotscher, M., Sakmann, B., 1997. Regulation of Synaptic Efficacy by  
1433 Coincidence of Postsynaptic APs and EPSPs. *Science* 275, 213–215.  
1434 <https://doi.org/10.1126/science.275.5297.213>
- 1435 Mehaffey, W.H., Doupe, A.J., 2015. Naturalistic stimulation drives opposing heterosynaptic  
1436 plasticity at two inputs to songbird cortex. *Nat. Neurosci.* 18, 1272–1280.  
1437 <https://doi.org/10.1038/nn.4078>
- 1438  
1439 Mihalas, S., 2011. Calcium messenger heterogeneity: a possible signal for spike timing-  
1440 dependent plasticity. *Front. Comput. Neurosci.* 4, 158.  
1441 <https://doi.org/10.3389/fncom.2010.00158>
- 1442 Min, R., Nevian, T., 2012. Astrocyte signaling controls spike timing-dependent depression at  
1443 neocortical synapses. *Nat. Neurosci.* 15, 746–753. <https://doi.org/10.1038/nn.3075>
- 1444 Mishra, R.K., Kim, S., Guzman, S.J., Jonas, P., 2016. Symmetric spike timing-dependent plasticity  
1445 at CA3–CA3 synapses optimizes storage and recall in autoassociative networks. *Nat. Commun.* 7.  
1446 <https://doi.org/10.1038/ncomms11552>
- 1447 Morrison, A., Diesmann, M., Gerstner, W., 2008. Phenomenological models of synaptic plasticity  
1448 based on spike timing. *Biol. Cybern.* 98, 459. <https://doi.org/10.1007/s00422-008-0233-1>
- 1449 Mu, Y., Poo, M., 2006. Spike Timing-Dependent LTP/LTD Mediates Visual Experience-Dependent  
1450 Plasticity in a Developing Retinotectal System. *Neuron* 50, 115–125.  
1451 <https://doi.org/10.1016/j.neuron.2006.03.009>
- 1452 Nakano, T., Yoshimoto, J., Doya, K., 2013. A model-based prediction of the calcium responses in  
1453 the striatal synaptic spines depending on the timing of cortical and dopaminergic inputs and  
1454 post-synaptic spikes. *Front. Comput. Neurosci.* 7, 119.  
1455 <https://doi.org/10.3389/fncom.2013.00119>
- 1456 Neve, K.A., Seamans, J.K., Trantham-Davidson, H., 2004. Dopamine Receptor Signaling. *J. Recept.*  
1457 *Signal Transduct.* 24, 165–205. <https://doi.org/10.1081/RRS-200029981>
- 1458 Nevian, T., Sakmann, B., 2006. Spine Ca<sup>2+</sup> Signaling in Spike-Timing-Dependent Plasticity. *J.*  
1459 *Neurosci.* 26, 11001–11013. <https://doi.org/10.1523/JNEUROSCI.1749-06.2006>
- 1460 Nishiyama, M., Hong, K., Mikoshiba, K., Poo, M., Kato, K., 2000. Calcium stores regulate the  
1461 polarity and input specificity of synaptic modification. *Nature* 408, 584–588.  
1462 <https://doi.org/10.1038/35046067>
- 1463 Nishiyama, M., Togashi, K., Aihara, T., Hong, K., 2010. GABAergic Activities Control Spike Timing-  
1464 and Frequency-Dependent Long-Term Depression at Hippocampal Excitatory Synapses. *Front.*  
1465 *Synaptic Neurosci.* 2. <https://doi.org/10.3389/fnsyn.2010.00022>

- 1466 Oliveira, J.F., Sardinha, V.M., Guerra-Gomes, S., Araque, A., Sousa, N., 2015. Do stars govern our  
1467 actions? Astrocyte involvement in rodent behavior. *Trends Neurosci.* 38, 535–549.  
1468 <https://doi.org/10.1016/j.tins.2015.07.006>
- 1469 Paille, V., Fino, E., Du, K., Morera-Herreras, T., Perez, S., Kotaleski, J.H., Venance, L., 2013.  
1470 GABAergic Circuits Control Spike-Timing-Dependent Plasticity. *J. Neurosci.* 33, 9353–9363.  
1471 <https://doi.org/10.1523/JNEUROSCI.5796-12.2013>
- 1472 Panatier, A., Theodosis, D.T., Mothet, J.-P., Touquet, B., Pollegioni, L., Poulain, D.A., Oliet, S.H.R.,  
1473 2006. Glia-derived D-serine controls NMDA receptor activity and synaptic memory. *Cell* 125,  
1474 775–784. <https://doi.org/10.1016/j.cell.2006.02.051>
- 1475 Pascual, O., Casper, K.B., Kubera, C., Zhang, J., Revilla-Sanchez, R., Sul, J.-Y., Takano, H., Moss, S.J.,  
1476 McCarthy, K., Haydon, P.G., 2005. Astrocytic purinergic signaling coordinates synaptic networks.  
1477 *Science* 310, 113–116. <https://doi.org/10.1126/science.1116916>
- 1478 Park, H., Poo, M., 2013. Neurotrophin regulation of neural circuit development and function. *Nat.*  
1479 *Rev. Neurosci.* 14, 7–23. <https://doi.org/10.1038/nrn3379>
- 1480 Pattwell S.S., Bath K.G., Perez-Castro R., Lee F.S., Chao M.V., Ninan I., 2012. The BDNF Val66Met  
1481 polymorphism impairs synaptic transmission and plasticity in the infralimbic medial prefrontal  
1482 cortex. *J. Neurosci.* 32, 2410–2421. <https://doi.org/10.1523/JNEUROSCI.5205-11.2012>.
- 1483 Pawlak, V., Kerr, J.N.D., 2008. Dopamine Receptor Activation Is Required for Corticostriatal  
1484 Spike-Timing-Dependent Plasticity. *J. Neurosci.* 28, 2435–2446.  
1485 <https://doi.org/10.1523/JNEUROSCI.4402-07.2008>
- 1486 Pawlak, V., Wickens, J.R., Kirkwood, A., Kerr, J.N.D., 2010. Timing is not Everything:  
1487 Neuromodulation Opens the STDP Gate. *Front. Synaptic Neurosci.* 2.  
1488 <https://doi.org/10.3389/fnsyn.2010.00146>
- 1489 Pi, H.J., Lisman, J.E., 2008. Coupled phosphatase and kinase switches produce the tristability  
1490 required for long-term potentiation and long-term depression. *J. Neurosci. Off. J. Soc. Neurosci.*  
1491 28, 13132–13138. <https://doi.org/10.1523/JNEUROSCI.2348-08.2008>
- 1492 Plotkin, J.L., Shen, W., Rafalovich, I., Sebel, L.E., Day, M., Chan, C.S., Surmeier, D.J., 2013.  
1493 Regulation of dendritic calcium release in striatal spiny projection neurons. *J. Neurophysiol.*  
1494 110, 2325–2336. <https://doi.org/10.1152/jn.00422.2013>
- 1495 Poirazi, P., Brannon, T., Mel, B.W., 2003. Arithmetic of subthreshold synaptic summation in a  
1496 model CA1 pyramidal cell. *Neuron* 37, 977–987.
- 1497 Rachmuth, G., Shouval, H.Z., Bear, M.F., Poon, C.-S., 2011. A biophysically-based neuromorphic  
1498 model of spike rate- and timing-dependent plasticity. *Proc. Natl. Acad. Sci.* 108, E1266–E1274.  
1499 <https://doi.org/10.1073/pnas.1106161108>
- 1500 Ramos, B.P., Arnsten, A.F.T., 2007. Adrenergic pharmacology and cognition: Focus on the  
1501 prefrontal cortex. *Pharmacol. Ther.* 113, 523–536.  
1502 <https://doi.org/10.1016/j.pharmthera.2006.11.006>

- 1503 Rebola, N., Carta, M., Lanore, F., Blanchet, C., Mulle, C., 2011. NMDA receptor-dependent  
1504 metaplasticity at hippocampal mossy fiber synapses. *Nat. Neurosci.* 14, 691–693.  
1505 <https://doi.org/10.1038/nn.2809>
- 1506 Rodríguez-Moreno, A., Paulsen, O., 2008. Spike timing-dependent long-term depression  
1507 requires presynaptic NMDA receptors. *Nat. Neurosci.* 11, 744–745.  
1508 <https://doi.org/10.1038/nn.2125>
- 1509 Ruan, H., Saur, T., Yao, W.-D., 2014. Dopamine-enabled anti-Hebbian timing-dependent plasticity  
1510 in prefrontal circuitry. *Front. Neural Circuits* 8. <https://doi.org/10.3389/fncir.2014.00038>
- 1511 Rubin, J.E., Gerkin, R.C., Bi, G.-Q., Chow, C.C., 2005. Calcium time course as a signal for spike-  
1512 timing-dependent plasticity. *J. Neurophysiol.* 93, 2600–2613.  
1513 <https://doi.org/10.1152/jn.00803.2004>
- 1514 Safo, P., Regehr, W.G., 2008. Timing dependence of the induction of cerebellar LTD.  
1515 *Neuropharmacology* 54, 213–218. <https://doi.org/10.1016/j.neuropharm.2007.05.029>
- 1516 Sahlender, D.A., Savtchouk, I., Volterra, A., 2014. What do we know about gliotransmitter release  
1517 from astrocytes? *Philos. Trans. R. Soc. Lond. B. Biol. Sci.* 369, 20130592.  
1518 <https://doi.org/10.1098/rstb.2013.0592>
- 1519 Sakata K., Woo N.H., Martinowich K., Greene J.S., Schloesser R.J., Shen L., Lu B., 2009. Critical role  
1520 of promoter IV-driven BDNF transcription in GABAergic transmission and synaptic plasticity in  
1521 the prefrontal cortex. *Proc. Natl. Acad. Sci. USA.* 14, 5942-5947.  
1522 <https://doi.org/10.1073/pnas.0811431106>
- 1523 Salgado, H., Köhr, G., Treviño, M., 2012. Noradrenergic ‘Tone’ Determines Dichotomous Control  
1524 of Cortical Spike-Timing-Dependent Plasticity. *Sci. Rep.* 2. <https://doi.org/10.1038/srep00417>
- 1525 Saudargienė, A., Graham, B.P., 2015. Inhibitory control of site-specific synaptic plasticity in a  
1526 model CA1 pyramidal neuron. *Biosystems* 130, 37–50.  
1527 <https://doi.org/10.1016/j.biosystems.2015.03.001>
- 1528 Schultz, W., 2007. Behavioral dopamine signals. *Trends Neurosci.* 30, 203–210.  
1529 <https://doi.org/10.1016/j.tins.2007.03.007>
- 1530 Schulz, J.M., Redgrave, P., Reynolds, J.N.J., 2010. Cortico-Striatal Spike-Timing Dependent  
1531 Plasticity After Activation of Subcortical Pathways. *Front. Synaptic Neurosci.* 2.  
1532 <https://doi.org/10.3389/fnsyn.2010.00023>
- 1533 Scimemi, A., 2014. Structure, function, and plasticity of GABA transporters. *Front. Cell. Neurosci.*  
1534 8, 161. <https://doi.org/10.3389/fncel.2014.00161>
- 1535 Seol, G.H., Ziburkus, J., Huang, S., Song, L., Kim, I.T., Takamiya, K., Huganir, R.L., Lee, H.-K.,  
1536 Kirkwood, A., 2007. Neuromodulators Control the Polarity of Spike-Timing-Dependent Synaptic  
1537 Plasticity. *Neuron* 55, 919. <https://doi.org/10.1016/j.neuron.2007.08.013>
- 1538 Shen, W., Flajolet, M., Greengard, P., Surmeier, D.J., 2008. Dichotomous Dopaminergic Control of  
1539 Striatal Synaptic Plasticity. *Science* 321, 848–851. <https://doi.org/10.1126/science.1160575>

- 1540 Shim, Y., Philippides, A., Staras, K., Husbands, P., 2016. Unsupervised Learning in an Ensemble of  
1541 Spiking Neural Networks Mediated by ITDP. *PLoS Comput. Biol.* 12, e1005137.  
1542 <https://doi.org/10.1371/journal.pcbi.1005137>  
1543
- 1544 Shouval, H.Z., Bear, M.F., Cooper, L.N., 2002. A unified model of NMDA receptor-dependent  
1545 bidirectional synaptic plasticity. *Proc. Natl. Acad. Sci. U. S. A.* 99, 10831–10836.  
1546 <https://doi.org/10.1073/pnas.152343099>
- 1547 Shouval, H.Z., Kalantzis, G., 2005. Stochastic properties of synaptic transmission affect the shape  
1548 of spike time-dependent plasticity curves. *J. Neurophysiol.* 93, 1069–1073.  
1549 <https://doi.org/10.1152/jn.00504.2004>
- 1550 Sjöström, P.J., Rancz, E.A., Roth, A., Häusser, M., 2008. Dendritic Excitability and Synaptic  
1551 Plasticity. *Physiol. Rev.* 88, 769–840. <https://doi.org/10.1152/physrev.00016.2007>
- 1552 Sjöström, P.J., Turrigiano, G.G., Nelson, S.B., 2003. Neocortical LTD via Coincident Activation of  
1553 Presynaptic NMDA and Cannabinoid Receptors. *Neuron* 39, 641–654.  
1554 [https://doi.org/10.1016/S0896-6273\(03\)00476-8](https://doi.org/10.1016/S0896-6273(03)00476-8)
- 1555 Sjöström, P.J., Turrigiano, G.G., Nelson, S.B., 2001. Rate, timing, and cooperativity jointly  
1556 determine cortical synaptic plasticity. *Neuron* 32, 1149–1164.
- 1557 Standage, D., Trappenberg, T., Blohm, G., 2014. Calcium-dependent calcium decay explains STDP  
1558 in a dynamic model of hippocampal synapses. *PloS One* 9, e86248.  
1559 <https://doi.org/10.1371/journal.pone.0086248>
- 1560 Sugisaki, E., Fukushima, Y., Fujii, S., Yamazaki, Y., Aihara, T., 2016. The effect of coactivation of  
1561 muscarinic and nicotinic acetylcholine receptors on LTD in the hippocampal CA1 network. *Brain*  
1562 *Res.* 1649, Part A, 44–52. <https://doi.org/10.1016/j.brainres.2016.08.024>
- 1563 Sugisaki, E., Fukushima, Y., Tsukada, M., Aihara, T., 2011. Cholinergic modulation on spike  
1564 timing-dependent plasticity in hippocampal CA1 network. *Neuroscience* 192, 91–101.  
1565 <https://doi.org/10.1016/j.neuroscience.2011.06.064>
- 1566 Sutton, R.S., Barto, A.G., 1998. Reinforcement learning: an introduction. Cambridge, MA: MIT  
1567 Press.
- 1568 Takkala, P., Woodin, M.A., 2013. Muscarinic acetylcholine receptor activation prevents  
1569 disinhibition-mediated LTP in the hippocampus. *Front. Cell. Neurosci.* 7.  
1570 <https://doi.org/10.3389/fncel.2013.00016>
- 1571 Thiele, A., 2013. Muscarinic signaling in the brain. *Annu. Rev. Neurosci.* 36, 271–294.  
1572 <https://doi.org/10.1146/annurev-neuro-062012-170433>
- 1573 Tzounopoulos, T., Kim, Y., Oertel, D., Trussell, L.O., 2004. Cell-specific, spike timing-dependent  
1574 plasticities in the dorsal cochlear nucleus. *Nat. Neurosci.* 7, 719–725.  
1575 <https://doi.org/10.1038/nn1272>
- 1576 Urakubo, H., Honda, M., Froemke, R.C., Kuroda, S., 2008. Requirement of an Allosteric Kinetics of  
1577 NMDA Receptors for Spike Timing-Dependent Plasticity. *J. Neurosci.* 28, 3310–3323.  
1578 <https://doi.org/10.1523/JNEUROSCI.0303-08.2008>

1579 Valtcheva, S., Paillé, V., Dembitskaya, Y., Perez, S., Gangarossa, G., Fino, E., Venance, L., 2017.  
1580 Developmental control of spike-timing-dependent plasticity by tonic GABAergic signaling in  
1581 striatum. *Neuropharmacology* 121, 261–277.  
1582 <https://doi.org/10.1016/j.neuropharm.2017.04.012>

1583 Valtcheva, S., Venance, L., 2016. Astrocytes gate Hebbian synaptic plasticity in the striatum. *Nat.*  
1584 *Commun.* 7. <https://doi.org/10.1038/ncomms13845>

1585 Verkhratsky, A., Matteoli, M., Parpura, V., Mothet, J.-P., Zorec, R., 2016. Astrocytes as secretory  
1586 cells of the central nervous system: idiosyncrasies of vesicular secretion. *EMBO J.* 35, 239–257.  
1587 <https://doi.org/10.15252/embj.201592705>

1588 Wang, S.H., Redondo, R.L, Morris, R.G., 2010. Relevance of synaptic tagging and capture to the  
1589 persistence of long-term potentiation and everyday spatial memory. *Proc. Natl. Acad. Sci. U.S.A.*  
1590 107, 19537-19542. <https://doi.org/10.1073/pnas.1008638107>

1591 Williams, S.R., Wozny, C., Mitchell, S.J., 2007. The back and forth of dendritic plasticity. *Neuron.*  
1592 56, 947-953. <https://doi.org/10.1016/j.neuron.2007.12.004>

1593 Wittenberg, G.M., Wang, S.S.-H., 2006. Malleability of Spike-Timing-Dependent Plasticity at the  
1594 CA3–CA1 Synapse. *J. Neurosci.* 26, 6610–6617. <https://doi.org/10.1523/JNEUROSCI.5388-05.2006>

1595 Woodin, M.A., Ganguly, K., Poo, M., 2003. Coincident pre- and postsynaptic activity modifies  
1596 GABAergic synapses by postsynaptic changes in Cl<sup>-</sup> transporter activity. *Neuron* 39, 807–820.

1600 Xu, T.-X., Yao, W.-D., 2010. D1 and D2 dopamine receptors in separate circuits cooperate to drive  
1601 associative long-term potentiation in the prefrontal cortex. *Proc. Natl. Acad. Sci. U. S. A.* 107,  
1602 16366. <https://doi.org/10.1073/pnas.1004108107>

1603 Yagishita, S., Hayashi-Takagi, A., Ellis-Davies, G.C.R., Urakubo, H., Ishii, S., Kasai, H., 2014. A  
1604 critical time window for dopamine actions on the structural plasticity of dendritic spines.  
1605 *Science* 345, 1616–1620. <https://doi.org/10.1126/science.1255514>

1606 Yang, K., Dani, J.A., 2014. Dopamine D1 and D5 Receptors Modulate Spike Timing-Dependent  
1607 Plasticity at Medial Perforant Path to Dentate Granule Cell Synapses. *J. Neurosci.* 34, 15888–  
1608 15897. <https://doi.org/10.1523/JNEUROSCI.2400-14.2014>

1609 Yin, H.H., Knowlton, B.J., 2006. The role of the basal ganglia in habit formation. *Nat. Rev.*  
1610 *Neurosci.* 7, 464–476. <https://doi.org/10.1038/nrn1919>

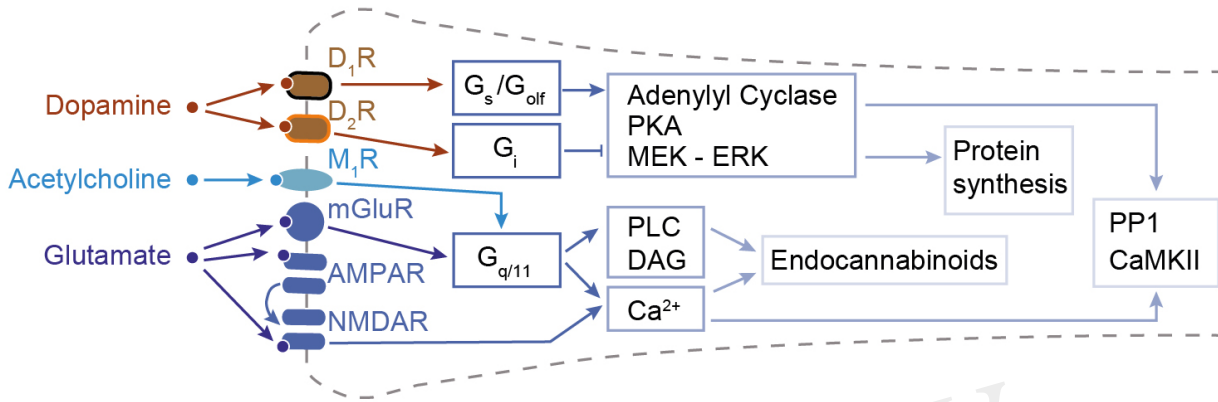
1611 Zhang, J.-C., Lau, P.-M., Bi, G.-Q., 2009. Gain in sensitivity and loss in temporal contrast of STDP  
1612 by dopaminergic modulation at hippocampal synapses. *Proc. Natl. Acad. Sci. U. S. A.* 106, 13028.  
1613 <https://doi.org/10.1073/pnas.0900546106>

1614 Zhang, Z., Gong, N., Wang, W., Xu, L., Xu, T.-L., 2008. Bell-shaped D-serine actions on  
1615 hippocampal long-term depression and spatial memory retrieval. *Cereb. Cortex N. Y. N* 1991 18,  
1616 2391–2401. <https://doi.org/10.1093/cercor/bhn008>

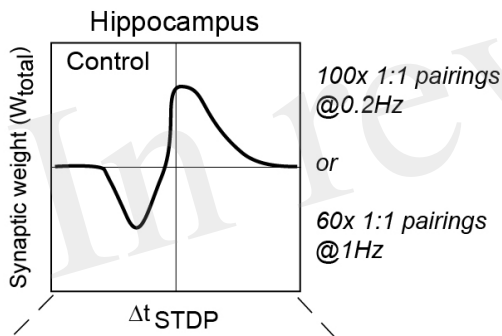
1617

Figure 1.JPEG

**a**

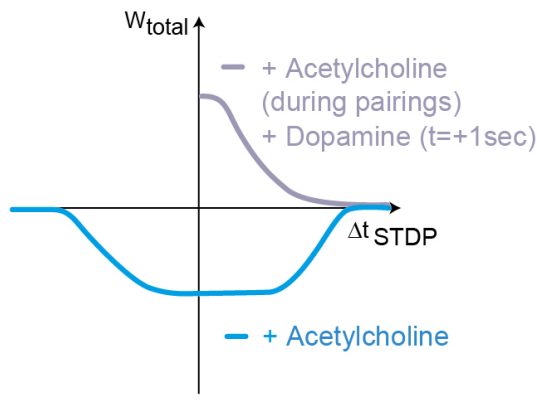
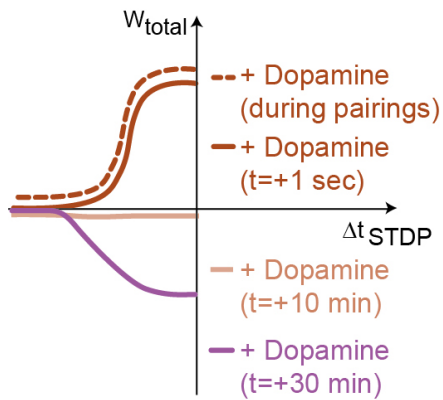


**b**

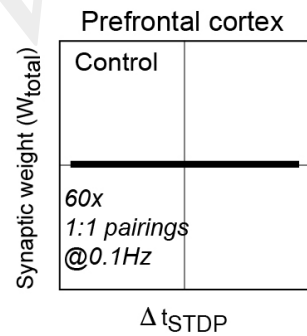


(1)

(2)



**c**



(1)

(2)

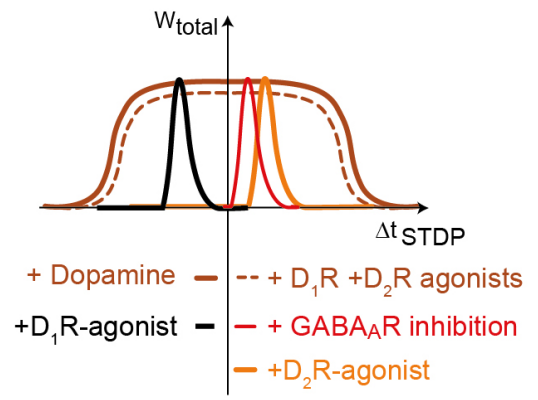


Figure 2.JPEG

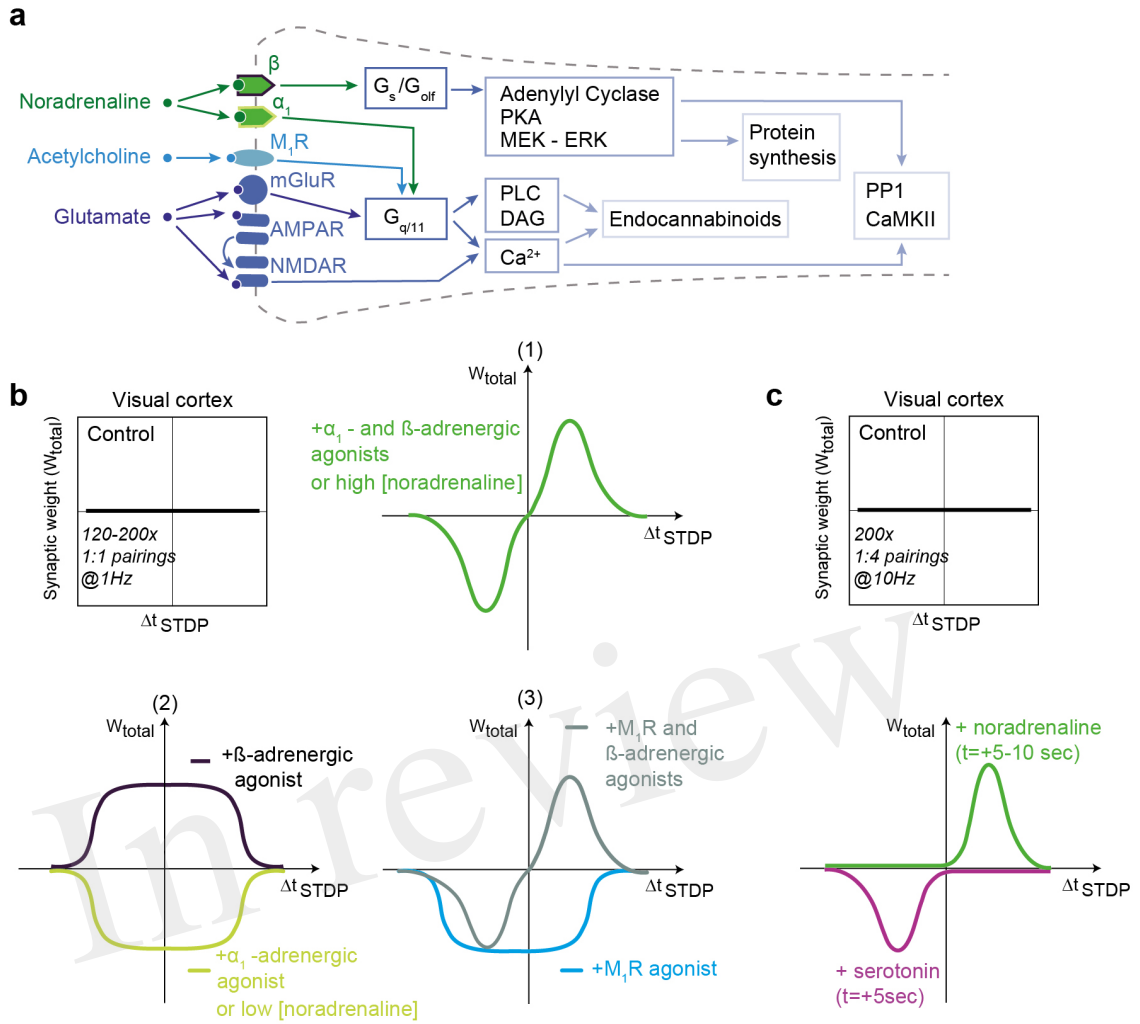


Figure 3.JPEG

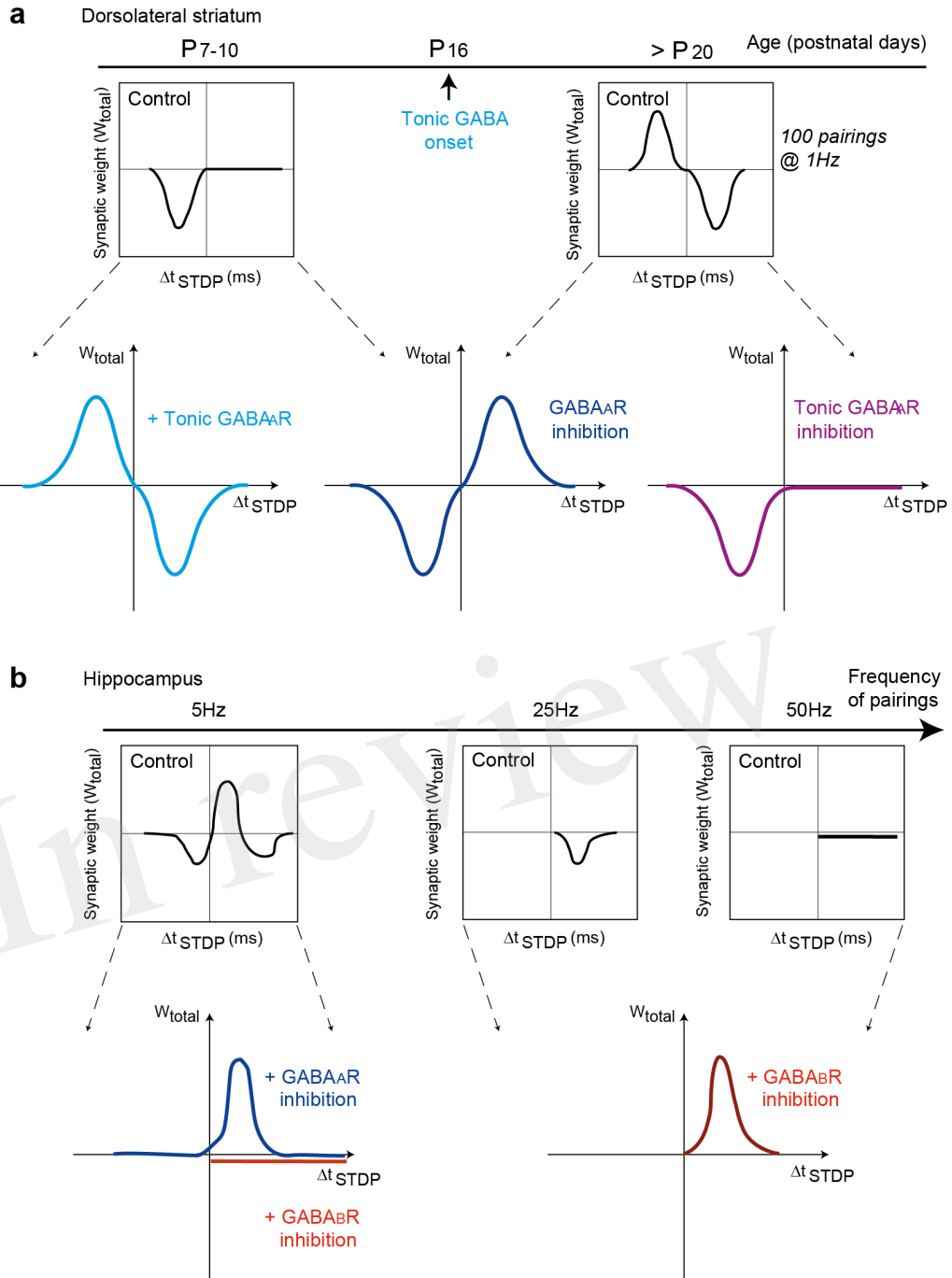


Figure 4.JPEG

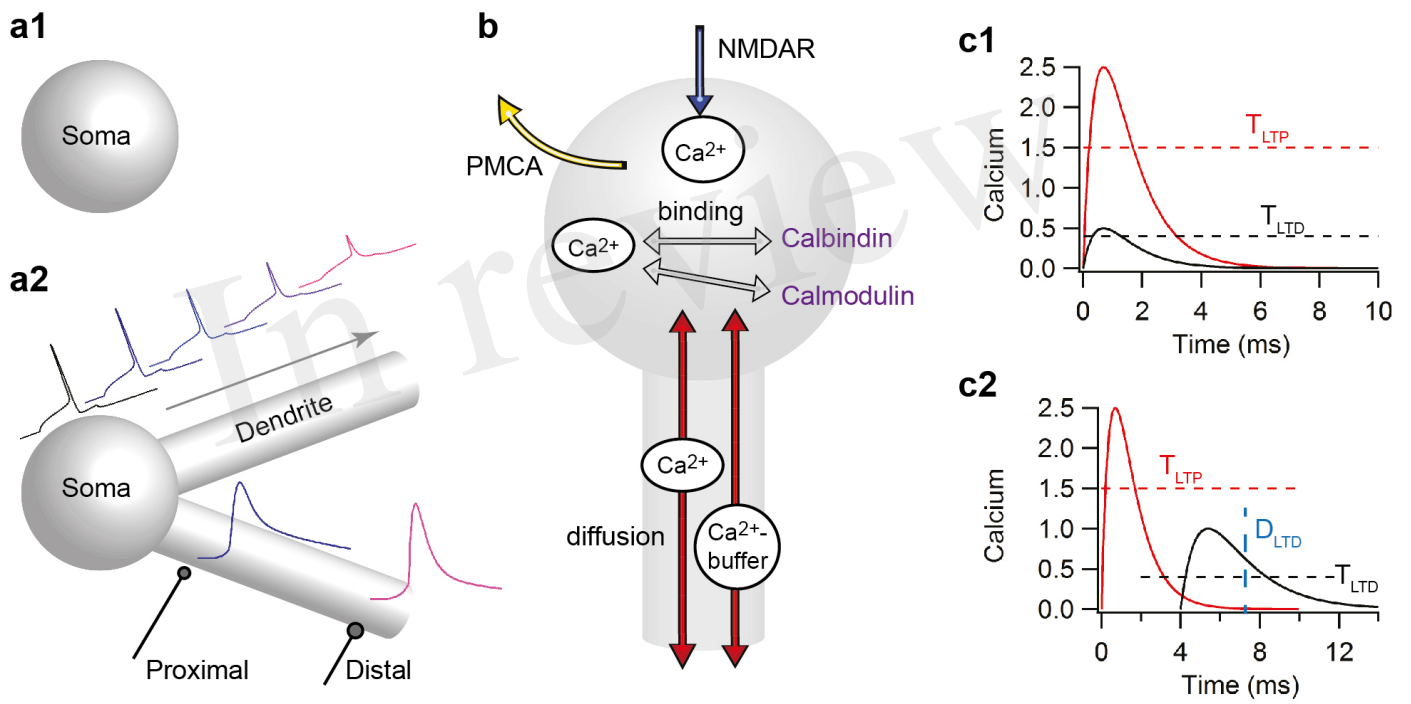


Figure 5.JPEG

